# PRECISION MEASUREMENTS AT LEP AND LEP-2

Tatsuo Kawamoto
International Center for Elementary Particle Physics, University of Tokyo
Hongo 7-3-1, Bunkyo-ku, Tokyo 113, Japan

Representing the LEP Collaborations

ABSTRACT

The status of the LEP precision measurements is reviewed, covering the electroweak measurements at the $Z^0$, the studies of fermion pair production, and the totally new subject of W physics at LEP-2. The results presented here include both published and preliminary ones. These precision results are used to check the overall consistency of the Standard Model, and in its framework, constraints on its parameters are derived. For some of the topics, some details of the experimental procedure are also discussed.

# 1 Introduction

A major subject of the LEP $e^+e^-$ collider at CERN is to explore the Standard Model in a precise and systematic manner. An $e^+e^-$ collider with the center-of-mass energy sufficient to cover all known gauge bosons, $\gamma$, $Z^0$, $W^\pm$, and the gluon, allows precision studies of the interaction of these particles with fermions, as well as among themselves. The Higgs particle, another key element of the Standard Model which is based on the spontaneously broken SU(2)×U(1) gauge symmetry, is not yet discovered. If the mass of the Higgs boson is within the range of the ever-increasing collision energy of LEP, it will be discovered, and once discovered, study of the nature of the Higgs boson will become a highlight of LEP. The LEP machine is the $e^+e^-$ energy frontier. The collision energy has been increasing since 1995. Direct searches for new particles and new phenomena, together with precision tests of the expectations from the Standard Model, provide stringent tests of possible new physics beyond the Standard Model.

Here the status of LEP precision measurements is reviewed, and implications for the Standard Model are discussed.

Since the start of operation in 1989, LEP has run at the center-of-mass energy near to the mass of the $Z^0$. The four LEP experiments, ALEPH, DELPHI, L3, and OPAL, each collected over four million $Z^0$ decay events. Based on these data, the properties of the $Z^0$ have been measured with very high accuracy. Hadronic decay of the $Z^0$ provides a high-statistics quark pair sample of high purity, which is very good for the study of QCD.

At the end of 1995, the energy upgrade of the LEP machine started. After about 5 $pb^{-1}$ of data was collected at $\sqrt{s}$ = 130–140 GeV, the center-of-mass energy reached 161 GeV in 1996, which is above the nominal threshold of W pair production. This is commonly referred to as the LEP-2 program. Each experiment collected about 10 $pb^{-1}$ of integrated luminosity. The LEP energy further increased and data were collected at 172 GeV (10 $pb^{-1}$) in 1996 and at 183 GeV (60 $pb^{-1}$) in 1997.

The results presented here are based mainly on the data collected up to 1996 by the LEP Collaborations. Some of the results are preliminary.

## 2 The $Z^0$

In $e^+e^-$ collisions, the $Z^0$ boson forms an $s$-channel resonance. The cross section is large at center-of-mass energy near the mass of the $Z^0$, $m_Z$. In the first phase of LEP, the collision energy was set near $m_Z$ and a large number of $Z^0$ decay events were collected.

In the Standard Model, at tree level, three parameters are needed to calculate the electroweak quantities. For the analyses of the $Z^0$ data, the following set of three precisely known quantities $(\alpha_{\rm em}, G_\mu, m_Z)$ is used. These are the electromagnetic coupling constant, the muon decay constant (Fermi constant), and the mass of the $Z^0$ boson, respectively. For the calculation of higher-order corrections, the mass of the top quark $(m_t)$ and the Higgs boson $(m_H)$, and the strong coupling constant $(\alpha_s)$ are also needed. Many of the higher-order corrections due to light fermions are incorporated by the use of running $\alpha_{\rm em}(s)$. There has been great progress in the precision calculation of the electroweak and QCD radiative corrections, and also in the QED corrections which are necessary to predict the observed quantities in the presence of initial-state radiation and other photonic effects.[1]

The cross section for fermion pair production viz $s$-channel exchanges of $\gamma$ and $Z^0$ has the following form:*

$$\begin{aligned} \frac{2s}{\pi\alpha^2 N_c}\cdot\frac{d\sigma_f}{d\cos\theta} &= Q_f^2(1+\cos^2\theta) \\ &+ 4{\rm Re}[\chi({\rm s})][{\rm C}^{\rm s}_{\gamma Z}(1+\cos^2\theta)+2{\rm C}^{\rm a}_{\gamma Z}\cos\theta] \\ &+ 16|\chi(s)|^2[C^s_{ZZ}(1+\cos^2\theta)+8C^a_{ZZ}\cos\theta] \end{aligned} \tag{1}$$

with

$$\chi(s)=\frac{G_\mu m_Z^2}{8\pi\alpha\sqrt{2}}\cdot\frac{s}{(s-m_Z^2)+i(s\Gamma_Z/m_Z)} \quad .$$

Here, $\Gamma_Z$ is the total width of $Z^0$. The first term is from the photon exchange, the third term is due to the $Z^0$ exchange, and the second term comes from $\gamma-Z$ interference. The four coefficients $C^s_{\gamma Z}, C^a_{\gamma Z}, C^s_{ZZ}$, and $C^a_{ZZ}$ represent the terms symmetric "$s$" and antisymmetric "$a$" in $\cos\theta$. In terms of vector and axial vector couplings $g_V$ and $g_A$, these coefficients are given by

$$C^s_{\gamma Z}=g_{Ve}g_{Vf}, \quad C^a_{\gamma Z}=g_{Ae}g_{Af}, \tag{2}$$

$$C^s_{ZZ}=(g^2_{Ve}+g^2_{Ae})(g^2_{Vf}+g^2_{Af}), \quad C^a_{ZZ}=g_{Ve}g_{Ae}g_{Vf}g_{Af}. \tag{3}$$

*In this equation, the running of $\alpha$ is ignored for simplicity.

These couplings are related to the weak mixing angle $\sin^2\theta_{\rm eff}$ by

$$\begin{aligned} g_{V{\rm f}} &= \sqrt{\rho}(I_3 - 2Q_f \sin^2\theta_{\rm eff}), \\ g_{A{\rm f}} &= \sqrt{\rho} I_3. \end{aligned} \tag{4}$$

Here, both $\rho = 1 + \Delta\rho$ and $\sin^2\theta_{\rm eff}$ contain radiative corrections to the tree level definition.

The symmetric part of the $Z^0$ exchange term is related to the pole cross section $\sigma^0_{\rm f}$ and the partial decay width $\Gamma_{\rm ff}$ by

$$\sigma_{\rm f}(s) = \sigma^0_{\rm f} \frac{s\Gamma^2_{\rm Z}}{(s - m^2_{\rm Z})^2 + (s^2/m^2_{\rm Z})\Gamma^2_{\rm Z}} \tag{5}$$

with[†]

$$\sigma^0_{\rm f} = \frac{12\pi}{m^2_{\rm Z}} \cdot \frac{\Gamma_{\rm ee}\Gamma_{\rm ff}}{\Gamma^2_{\rm Z}}. \tag{6}$$

The antisymmetric terms produce the forward-backward charge asymmetry $A_{\rm FB}$. The contribution from the $\gamma$−Z interference term to $A_{\rm FB}$ is zero at $\sqrt{s} = m_{\rm Z}$, while the remaining asymmetry $A^0_{\rm FB}$ from the $Z^0$ exchange part at the resonance peak is given by

$$A^0_{\rm FB} = \frac{3}{4}\mathcal{A}_{\rm e}\mathcal{A}_{\rm f}, \tag{7}$$

where

$$\mathcal{A}_{\rm f} = \frac{2g_{V{\rm f}}g_{A{\rm f}}}{g^2_{V{\rm f}} + g^2_{A{\rm f}}} = \frac{2g_{V{\rm f}}/g_{A{\rm f}}}{1 + (g_{V{\rm f}}/g_{A{\rm f}})^2}. \tag{8}$$

Hence, $A^0_{\rm FB}$ is a sensitive quantity to determine the effective weak mixing angle $\sin^2\theta^{\rm lept}_{\rm eff}$, which is defined as

$$\sin^2\theta^{\rm lept}_{\rm eff} = \frac{1}{4}(1 - \frac{g_{V\ell}}{g_{A\ell}}). \tag{9}$$

While the partial width itself carries information on the higher-order electroweak corrections which depend on $m_{\rm t}$ and $m_{\rm H}$, partial width ratios have interesting properties because many of the universal corrections cancel.

[†]The partial widths include corrections due to final-state radiation (and QCD corrections in case of quarks). The $\sigma_0$ defined here differs from the actual pole cross section by the final-state correction on $\Gamma_{\rm ee}$.

The invisible $Z^0$ decay width $\Gamma_{\rm inv}$ is defined by

$$\Gamma_{\rm inv} \;=\; \Gamma_{\rm Z} - \Gamma_{\rm had} - 3\Gamma_{\ell\ell}. \tag{10}$$

In the Standard Model, $\Gamma_{\rm inv} = N_\nu \Gamma_{\nu\nu}$ and the ratio $\Gamma_{\nu\nu}/\Gamma_{\ell\ell}$ has the least sensitivity to any of the electroweak parameters, so it is predicted very accurately. The number of light neutrino species $N_\nu$ can be determined from $\Gamma_{\rm inv}/\Gamma_{\ell\ell}$, and for a given number of $N_\nu = 3$, it provides an interesting test of the Standard Model.

The ratio of hadronic and leptonic widths $R_\ell = \Gamma_{\rm had}/\Gamma_{\ell\ell}$, which is determined by the ratio of hadronic and leptonic cross sections (and thus insensitive to the common luminosity error), is a quantity sensitive to the strong coupling constant $\alpha_s(m_{\rm Z}^2)$, because $\Gamma_{\rm had}$ contains the QCD correction of $(1 + \alpha_s/\pi + ...)$. It is also interesting to note that the leptonic pole cross section $\sigma^0_{\ell\ell}$ has even higher sensitivity. One can see this from the relation $\sigma^0_{\ell\ell} = (12\pi/m_{\rm Z}^2)(\Gamma_{\ell\ell}/\Gamma_{\rm Z})^2 = (12\pi/m_{\rm Z}^2)(R_\ell + 3 + 3\Gamma_{\nu\nu}/\Gamma_{\ell\ell})^{-2}$, which contains dependence on $R_\ell^2$ compared to the $R_\ell$ itself. Determination of $\alpha_s(m_{\rm Z}^2)$ from the $Z^0$ parameters therefore profits from the improved precision measurement of experimental luminosity.

The $Z^0$ decay partial width into the b quark has a unique dependence on the top quark mass due to the vertex correction involving the top quark and W boson. The partial width ratio $R_{\rm b} = \Gamma_{\rm b\bar{b}}/\Gamma_{\rm had}$ has a specific $m_{\rm t}$ dependence and virtually no dependence on $m_{\rm H}$ because the correction is universal to all quark flavors. The QCD corrections also largely cancel in the ratio. Therefore, $R_{\rm b}$ used to be an important quantity to determine the $m_{\rm t}$ from the $Z^0$ parameters free from the uncertainty on $m_{\rm H}$. Now that the $m_{\rm t}$ has been experimentally determined at the Tevatron,[2] there is very little ambiguity in the Standard Model value of $R_{\rm b}$; hence, the precise measurement of $R_{\rm b}$ is very worthwhile in testing the Standard Model. The ratio $R_{\rm c}$ is rather insensitive to the variation of $m_{\rm t}$ because the largest component of $\Gamma_{\rm had}$ has the same dependence as $\Gamma_{\rm c\bar{c}}$.

## 2.1 Lineshape and Lepton $A_{\rm FB}$

A set of precision measurements of basic quantities, cross sections for hadronic and leptonic final states, and leptonic forward-backward charge asymmetries provides rich information on the properties of the $Z^0$ and allows important tests of the Standard Model. The mass $m_{\rm Z}$ and the total width $\Gamma_{\rm Z}$ of the $Z^0$ are determined from the lineshape measurement, that is, by measuring the cross section for the

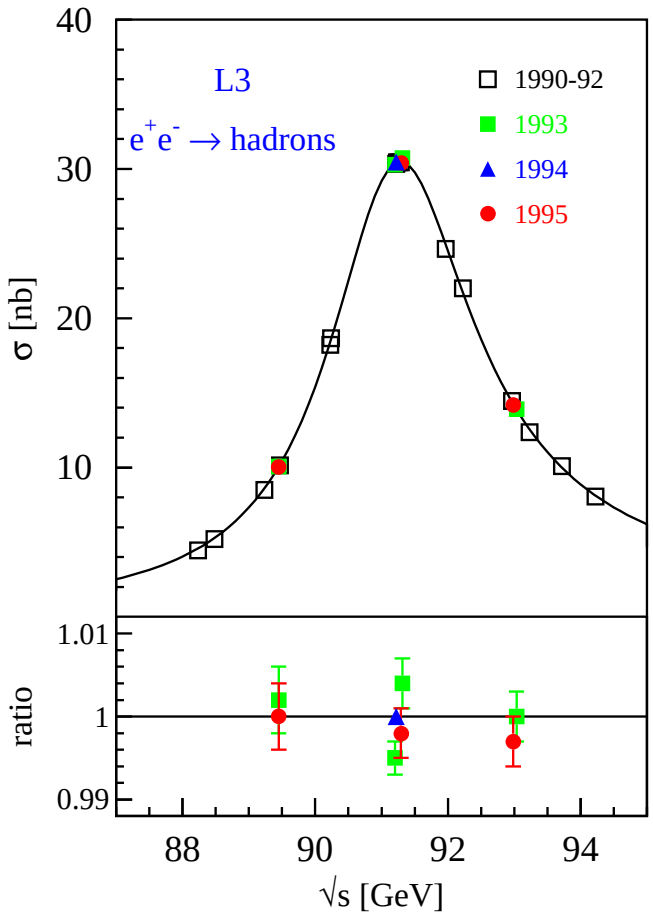


Fig. 1. A lineshape measurement.

process $e^+e^- \to f\bar{f}$ ($f\bar{f} = q\bar{q},\ \ell^+\ell^-$) as a function of center-of-mass energies around the $Z^0$ resonance at $\sqrt{s} \approx m_Z$ (Fig. 1). The accuracy of how well these parameters can be extracted depends on how accurately the "lineshape" is determined. Since the hadronic decay is a dominant decay mode of the $Z^0$, $m_Z$ and $\Gamma_Z$ are mainly determined from the measurement of the hadronic lineshape. Available $Z^0$ data samples of a typical LEP experiment are summarized in Table 1.

The data sample from 1993–1995 is particularly important. In 1993 and 1995, precision energy scans were performed at three center-of-mass energy points: on the resonance peak, and on two off-peak points approximately 1.8 GeV above and below $m_Z$. About 36 $pb^{-1}$ of integrated luminosity was collected by each experiment at these off-peak points, almost equally distributed to peak +2 and

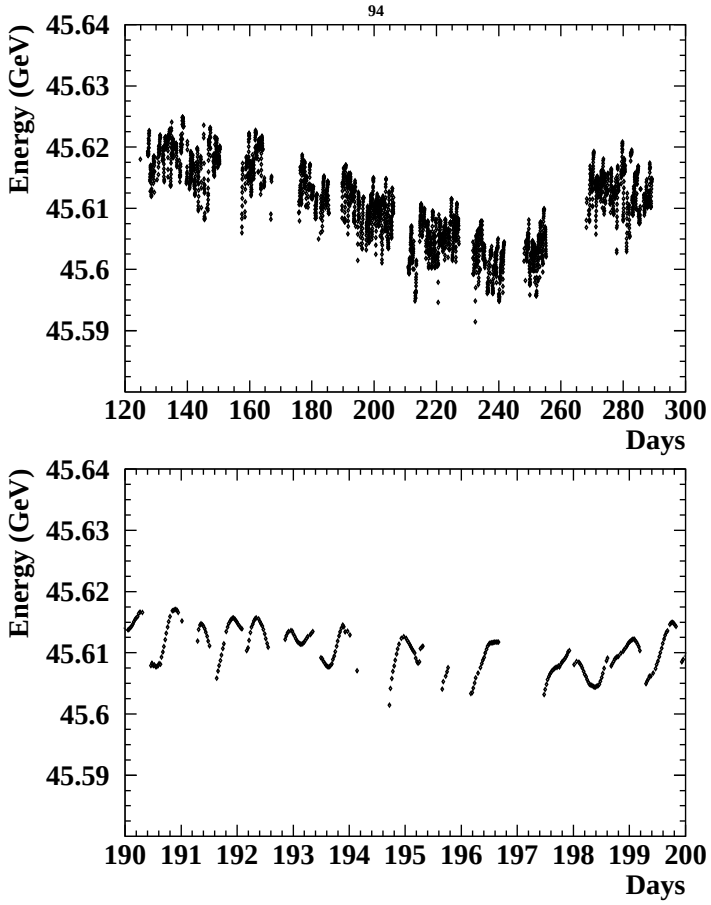


Fig. 2. A typical LEP energy history.

Table 1. Dataset of LEP run near the $Z^0$.

| Year | | $\int$Luminosity ($pb^{-1}$)/exp. | | |
|---|---|---|---|---|
| | | on-peak | off-peak | |
| 1989 | 11-point scan | 0.6 | 0.7 | |
| 1990 | 7-point scan | 3.5 | 3.1 | |
| 1991 | 5-point scan | 8 | 5 | |
| 1992 | peak | 25 | – | Published |
| 1993 | 3-point scan | 16 | 18 | Preliminary results |
| 1994 | peak | 55 | – | |
| 1995 | 3-point scan | 16 | 18 | |

peak $-2$ GeV points. In 1994, all data were collected on peak and about 55 $pb^{-1}$ was accumulated. The large off-peak luminosity is particularly important for the precise determination of $m_Z$ and $\Gamma_Z$. Measurements of absolute cross-section and lepton asymmetries benefited from the large data sample collected on peak in 1994. For an optimal use of these high-statistics samples, a number of improvements on the analyses have been made.

- The LEP energy calibration has been greatly improved.[3] The calibration is based on the resonant spin depolarization technique. A number of operational and environmental effects have been discovered which cause the beam energy to vary as a function of time, and the center-of-mass energies to be different at the four LEP experiments. Frequent resonant spin depolarization calibration of the beam energy and extensive monitoring of the LEP operating conditions allowed very precise tracking of the center-of-mass energy of $e^+e^-$ collisions over the time interval of the energy scans in 1993 and 1995, and for most of the on-peak runs in 1994. Now the LEP energy calibration has been finalized. An example of calibrated LEP beam energy as a function of time is shown in Fig. 2. The knowledge of the center-of-mass energy spread (about 50 MeV) has also been improved, which affects the observed cross section and hence the $\Gamma_Z$. The overall contributions of the LEP energy uncertainty to $m_Z$ and $\Gamma_Z$ are roughly 1.5 MeV and 1.5 MeV, respectively.

- The experimental luminosity is determined by measuring the small angle Bhabha scattering. The luminosity detectors of the LEP experiments had been upgraded by the time of these precision scans, and detailed analyses developed. An experimental accuracy of luminosity determination better than 0.1% has been achieved. Progress has also been made on the theoretical calculation of small angle Bhabha scattering,[4] and the theoretical uncertainty for the LEP luminosity measurement is now 0.11%.
- Over several years since the data have been collected, detailed analyses of hadronic and leptonic event selection have been performed and systematic errors have been largely reduced.

Using these data, lineshape parameters are extracted by fits using a theoretical parameterization of cross sections and lepton asymmetries. The standard set of these parameters are:

- $m_{\rm Z}$ and $\Gamma_{\rm Z}$;
- the hadronic pole cross section for $\rm Z^0$ exchange

$$\sigma^0_{\rm had} = \frac{12\pi}{m^2_{\rm Z}} \frac{\Gamma_{\rm ee}\Gamma_{\rm had}}{\Gamma^2_{\rm Z}};$$

- partial width ratios

$$R_{\rm e} = \Gamma_{\rm had}/\Gamma_{\rm ee}, \quad R_\mu = \Gamma_{\rm had}/\Gamma_{\mu\mu}, \quad R_\tau = \Gamma_{\rm had}/\Gamma_{\tau\tau};$$

- lepton pole asymmetries

$$A^{0,{\rm e}}_{\rm FB}, \quad A^{0,\mu}_{\rm FB}, \quad A^{0,\tau}_{\rm FB}.$$

Effects of radiative corrections are taken into account in the fitting procedure using semianalytical programs like ZFITTER.[5] The small contribution from the $\gamma-$Z interference term in the hadronic lineshape is constrained to the Standard Model value. An alternative approach where all the interference terms are determined by the data is discussed in the next section, together with the fermion pair analysis at LEP-2. Combined preliminary results[6] from the four LEP Collaborations for the lineshape parameters are summarized in Table 2.

The relative precision of the $m_{\rm Z}$ measurement is $2.2 \times 10^{-5}$, which is comparable to the precision of $G_\mu$ ($2 \times 10^{-5}$). The partial width ratios $R_\ell$ and $A^{0,\ell}_{\rm FB}$ determined for the three lepton species are consistent with lepton universality.

Table 2. Average lineshape and asymmetry parameters from the preliminary results of the four LEP Collaborations. The third column contains the results when lepton universality is assumed.

| Parameter | Average values | |
|---|---|---|
| | | lepton universality |
| $m_{\rm Z}$(GeV) | 91.1867 ± 0.0020 | 91.1867 ± 0.0020 |
| $\Gamma_{\rm Z}$(GeV) | 2.4948 ± 0.0025 | 2.4948 ± 0.0025 |
| $\sigma^0_{\rm had}$(nb) | 41.486 ± 0.053 | 41.486 ± 0.053 |
| $R_{\rm e}$ | 20.757 ± 0.056 | |
| $R_\mu$ | 20.783 ± 0.037 | |
| $R_\tau$ | 20.823 ± 0.050 | |
| $R_\ell$ | | 20.775 ± 0.027 |
| $A^{0,{\rm e}}_{\rm FB}$ | 0.0160 ± 0.0024 | |
| $A^{0,\mu}_{\rm FB}$ | 0.0163 ± 0.0014 | |
| $A^{0,\tau}_{\rm FB}$ | 0.0192 ± 0.0018 | |
| $A^{0,\ell}_{\rm FB}$ | | 0.0171 ± 0.0010 |

Note that $R_\tau$ is expected to be slightly larger ($\Gamma_{\tau\tau}$ smaller) than $R_{\rm e}$ and $R_\mu$ due to the large mass of the $\tau$ lepton, even if the couplings to $\rm Z^0$ are the same. When lepton universality is assumed, the set of nine parameters is reduced to five parameters, which are given in the third column of Table 2. Here, $R_\ell$ is defined by $R_\ell = \Gamma_{\rm had}/\Gamma_{\ell\ell}$, where $\Gamma_{\ell\ell}$ is the partial decay width of $\rm Z^0$ into a pair of massless charged leptons. The mass effect on $R_\tau$ has been corrected for the calculation of $R_\ell$. Figure 3 shows the 68% probability contours in the $R_\ell - A^{0,\ell}_{\rm FB}$ plane for each lepton species and for combined leptons assuming lepton universality.

The partial decay widths of the $\rm Z^0$ can be derived from the parameters in Table 2, and are summarized in Table 3. The ratio of invisible decay width to leptonic decay width is

$$\Gamma_{\rm inv}/\Gamma_{\ell\ell} \;=\; 5.960 \pm 0.022. \tag{11}$$

Using the Standard Model value of

$$(\Gamma_{\nu\nu}/\Gamma_{\ell\ell})_{\rm SM} \;=\; 1.991 \pm 0.001, \tag{12}$$

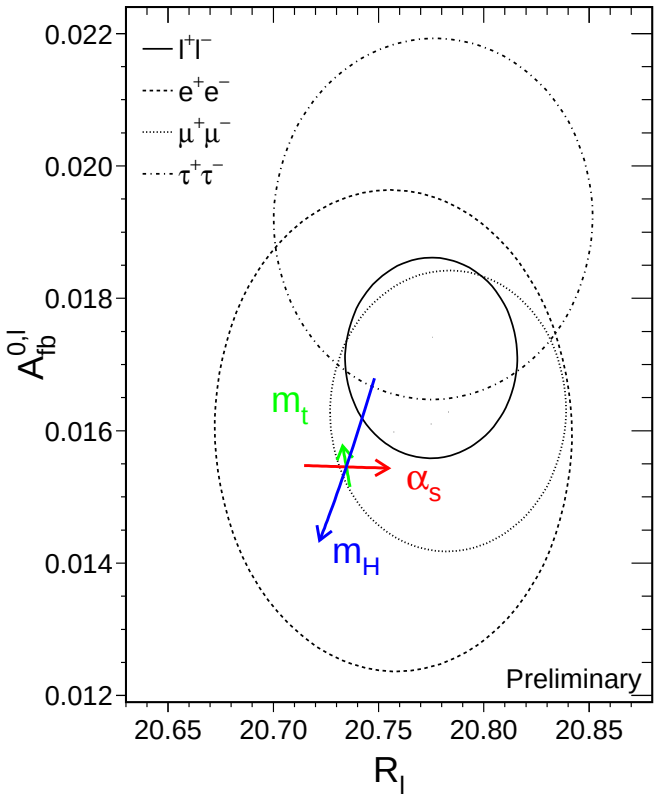


Fig. 3. Contour of 68% probability in the $R_\ell - A_{\rm FB}^{0,\ell}$ plane. The result for the $\tau$ lepton is corrected to the massless case. The arrows indicate the variations of the Standard Model expectation when $m_{\rm t}$, $m_{\rm H}$, and $\alpha_s(m_{\rm Z}^2)$ are varied in the intervals $175 \pm 5.5$ GeV, $300^{+700}_{-240}$, and $0.118 \pm 0.003$, respectively.

the number of light neutrino species is determined to be

$$N_\nu \;\; = \;\; 2.993 \pm 0.011. \tag{13}$$

As an alternative interpretation, assuming $N_\nu = 3$, the $\rm Z^0$ partial width for additional invisible decays is

$$\Delta\Gamma_{\rm inv} = -1.1 \pm 1.8 \;\; \text{MeV}, \;\; \text{or} \;\; \Delta\Gamma_{\rm inv} < 2.9 \;\; \text{MeV at the 95\% C.L.} \tag{14}$$

## 2.2 $\tau$ Polarization

The fermion pairs produced by $\rm e^+e^-$ collisions of the unpolarized LEP beams, $\rm e^+e^- \to Z^0 \to f\bar{f}$, are longitudinally polarized. In $\tau$ pair production, the polariza-

Table 3. The partial decay widths of the $Z^0$. In the case of lepton universality, $\Gamma_{\ell\ell}$ refers to the partial decay width into a pair of massless charged leptons.

| Parameter | Average values | |
|---|---|---|
| | | lepton universality |
| $\Gamma_{\rm had}$(MeV) | $1743.2 \pm 2.3$ | |
| $\Gamma_{\rm ee}$(MeV) | $83.94 \pm 0.14$ | |
| $\Gamma_{\mu\mu}$(MeV) | $83.84 \pm 0.20$ | |
| $\Gamma_{\tau\tau}$(MeV) | $83.68 \pm 0.24$ | |
| $\Gamma_{\ell\ell}$(MeV) | | $83.91 \pm 0.10$ |
| $\Gamma_{\rm inv}$(MeV) | | $500.1 \pm 1.8$ |

tion can be measured from the energy and angular distributions of the $\tau$ decay products. Here, the $\tau$ polarization is defined by

$$\mathcal{P}_\tau = \frac{\sigma_R - \sigma_L}{\sigma_R + \sigma_L}, \tag{15}$$

where $\sigma_R$ and $\sigma_L$ are the cross sections for $\tau$ pair production of a right-handed and left-handed $\tau^-$, respectively. The distribution of $\mathcal{P}_\tau$ as a function of the polar production angle of $\tau^-$ with respect to the beam $e^-$, at $\sqrt{s} = m_{\rm Z}$, is given using the coupling parameters $\mathcal{A}_\tau$ and $\mathcal{A}_{\rm e}$ by

$$\mathcal{P}_\tau(\cos\theta) = \frac{\mathcal{A}_\tau(1+\cos^2\theta) + 2\mathcal{A}_{\rm e}\cos\theta}{1+\cos^2\theta + 2\mathcal{A}_\tau\mathcal{A}_{\rm e}\cos\theta}. \tag{16}$$

By analyzing the angular dependence $\mathcal{P}_\tau(\cos\theta)$, $\mathcal{A}_\tau$ and $\mathcal{A}_{\rm e}$ are determined simultaneously with small correlation, allowing a test of universality of couplings of the $Z^0$ to $e$ and $\tau$.

Combined LEP results[6] for $\mathcal{A}_\tau$ and $\mathcal{A}_{\rm e}$ from measurements by the four collaborations, including recent preliminary results from DELPHI and L3, are:

$$\mathcal{A}_\tau = 0.1411 \pm 0.0064, \tag{17}$$

$$\mathcal{A}_{\rm e} = 0.1399 \pm 0.0073. \tag{18}$$

These are in agreement with lepton universality. A combined value assuming $e$-$\tau$ universality is

$$\mathcal{A}_\ell = 0.1406 \pm 0.0048. \tag{19}$$

## 2.3 Results from b and c Quarks

In the sample of hadronic $Z^0$ decays, one or more jets in an event originating from $b\overline{b}$ and $c\overline{c}$ can be tagged with good purity and efficiency. From these samples, information on the $Z^0$ partial widths into b and c quarks, and forward-backward asymmetries, are extracted. The relevant quantities discussed here are:

- the ratios of the b and c quark partial widths of the $Z^0$ to the total hadronic partial width, $R_b^0 = \Gamma_{b\overline{b}}/\Gamma_{had}$ and $R_c^0 = \Gamma_{c\overline{c}}/\Gamma_{had}$;
- the forward-backward asymmetries, $A_{FB}^{0,b}$ and $A_{FB}^{0,c}$.

The *lepton tag* is based on the weak decays of b/c hadrons to final states including leptons. These leptons tend to have high momentum ($p$), and the transverse momentum ($p_t$) with respect to the jet axis also tends to be large due to the large mass of the b/c hadrons. A well-established technique is the detection of muons and electrons with high $p, p_t$ in the hadronic event environment. The efficiency for the lepton tag is limited by the branching fraction of leptonic decay (roughly 10% to each lepton flavor). On the other hand, the leptons provide information about the quark charge, which can be used for the measurement of the forward-backward asymmetry. Separation between c and b quarks is made statistically on the basis of $p, p_t$. The lepton spectrum is fitted using expected distributions for $b \to \ell$, $b \to c \to \ell$, and $c \to \ell$, to derive the values of $R_b$, $R_c$, $A_{FB}^b$, and $A_{FB}^c$. The observed b asymmetry must be corrected for $B^0\bar{B}^0$ mixing. The average mixing can be obtained from LEP data by studying the like-sign and unlike-sign dilepton events. Many of the earlier heavy quark electroweak results from the LEP collaborations are based on the lepton analyses.

A powerful method of b tagging is based on the relatively long mean *lifetime* ($c\tau \approx 0.45$ mm), and large mean charged multiplicity of the b hadrons' decay. LEP detectors are equipped with precision vertex detectors which allow us to detect signatures of displaced decay vertices, either by directly reconstructing the vertex and measuring the decay length, or based on the large number of tracks with a significant impact parameter. A large *invariant mass* of the particles from the decay vertex is also an indication of b hadrons. Other useful information comes from the *event shape* of b jets, being different from that of lighter quarks.

Recent precise $R_b$ measurements use the *double-tag* technique. A hadronic event is divided into two hemispheres. In a sample of $N_{had}$ hadronic decays of the $Z^0$, the number of tagged hemisphere $N_t$ and the number of events $N_{tt}$ with both

hemispheres tagged are expressed in terms of $R_{\rm b}$ by

$$\frac{N_t}{2N_{\rm had}} = \varepsilon_{\rm b} R_{\rm b}, \tag{20}$$

$$\frac{N_{tt}}{N_{\rm had}} = \varepsilon_{\rm b}^2 R_{\rm b}, \tag{21}$$

where $\varepsilon_{\rm b}$ is the b-tagging efficiency per hemisphere. From these two equations we have

$$R_{\rm b} = \frac{N_t^2}{4 N_{tt} N_{\rm had}}. \tag{22}$$

In this way, we can determine the $R_{\rm b}$ without knowing the value of tagging efficiency. Note that $R_{\rm b}$ here is the ratio of cross sections, $R_{\rm b} = \sigma_{\rm b\overline{b}}/\sigma_{\rm had}$, which is slightly different from the partial width ratio $R_{\rm b}^0$ due mainly to the contribution of a photon exchange diagram for the quark pair production. The correction is evaluated using the Standard Model, and $R_{\rm b}^0 = R_{\rm b} + 0.0003$.

In a realistic experimental situation, however, the ideal relations above do not hold. When the contributions from background and possible correlation of tagging efficiency between hemispheres are considered, the basic equations are modified to

$$\frac{N_t}{2N_{\rm had}} = \varepsilon_{\rm b} R_{\rm b} + \varepsilon_{\rm c} R_{\rm c} + \varepsilon_{\rm uds}(1 - R_{\rm b} - R_{\rm c}), \tag{23}$$

$$\frac{N_{tt}}{N_{\rm had}} = C_{\rm b}\varepsilon_{\rm b}^2 R_{\rm b} + C_{\rm c}\varepsilon_{\rm c}^2 R_{\rm c} + C_{\rm uds}\varepsilon_{\rm uds}^2(1 - R_{\rm b} - R_{\rm c}); \tag{24}$$

here, $\varepsilon_{\rm c}$ and $\varepsilon_{\rm uds}$ are the tagging efficiency per hemisphere for c and light quark events, and the parameters $C$ account for the correlation of tagging efficiency between two hemispheres. These parameters have to be evaluated using a Monte Carlo or other methods. In order not to be very sensitive to the uncertainty on these parameters, the analyses are designed to keep the background contribution small (high purity b-tag: $\varepsilon_{\rm b} \gg \varepsilon_{\rm c} \gg \varepsilon_{\rm uds}$), and to avoid a large efficiency correlation between hemispheres ($C_{\rm b}$ very close to 1).

A number of different methods have been used to measure the value of $R_{\rm c}$. One method is the lepton analysis mentioned above. Recent analyses use: (1) an exclusive/inclusive double tag in which reconstructed $\rm D^{*\pm}$ mesons are used to measure the rate of $\rm c\overline{c}$ events, which depends on $R_{\rm c} P(\rm c\overline{c} \to D^{*+}) B(\rm D^{*+} \to \pi^+ D^0)$, and this is combined with the "slow pion tag" by detecting a low $p_t$ $\pi^+$ from $\rm D^{*+} \to \pi^+ D^0$ in the opposite hemisphere in order to constrain the product of

the branching ratios; (2) an inclusive/inclusive double tag using slow pions in order to gain efficiency, thus higher statistics, with a price of lower purity; (3) an exclusive/exclusive double tag using reconstructed $D^*$ and $D^0$ mesons to gain purity instead of a gain in the statistics; (4) a charm counting based on the rate of reconstructed $D^0$, $D^+$, $D_s$, and $\Lambda_c$, assuming that these are the major final states from the hadronization of $c\overline{c}$.

The forward-backward asymmetries for b and c quarks are measured using the lepton tag analyses, and also using D mesons for $A_{\rm FB}^{\rm c}$ (or both $A_{\rm FB}^{\rm c}$ and $A_{\rm FB}^{\rm b}$). The hemisphere jet charge technique has also been developed for the measurements of $A_{\rm FB}^{\rm b}$.

The results of these heavy flavor electroweak measurements from the four LEP collaborations are combined[6] in a consistent manner, taking into account the common systematic errors and correlations among the relevant quantities, and yielding the results summarized in Table 4. A set of measurements by the SLD Collaboration[7] of $R_{\rm b}$, and direct determination of $\mathcal{A}_{\rm b}$ and $\mathcal{A}_{\rm c}$ from the left-right forward-backward asymmetries using the polarized electron beam, are combined with the LEP results and also tabulated in Table 4.

Table 4. Combined results of heavy flavor electroweak measurements.

| Parameter | LEP data | LEP + SLD |
|---|---|---|
| $R_{\rm b}^0$ | $0.2174 \pm 0.0009$ | $0.2170 \pm 0.0009$ |
| $R_{\rm c}^0$ | $0.1727 \pm 0.0050$ | $0.1734 \pm 0.0048$ |
| $A_{\rm FB}^{0,{\rm b}}$ | $0.0983 \pm 0.0024$ | $0.0984 \pm 0.0024$ |
| $A_{\rm FB}^{0,{\rm c}}$ | $0.0739 \pm 0.0048$ | $0.0741 \pm 0.0048$ |
| $\mathcal{A}_{\rm b}$ | | $0.900 \pm 0.050$ |
| $\mathcal{A}_{\rm c}$ | | $0.650 \pm 0.058$ |

The errors on $R_{\rm b}$ and $R_{\rm c}$ are correlated since they are background to each other. Figure 4 shows the contours in the $R_{\rm b} - R_{\rm c}$ plane derived from the LEP + SLD data. The measured result is now consistent with the Standard Model to about one standard deviation.

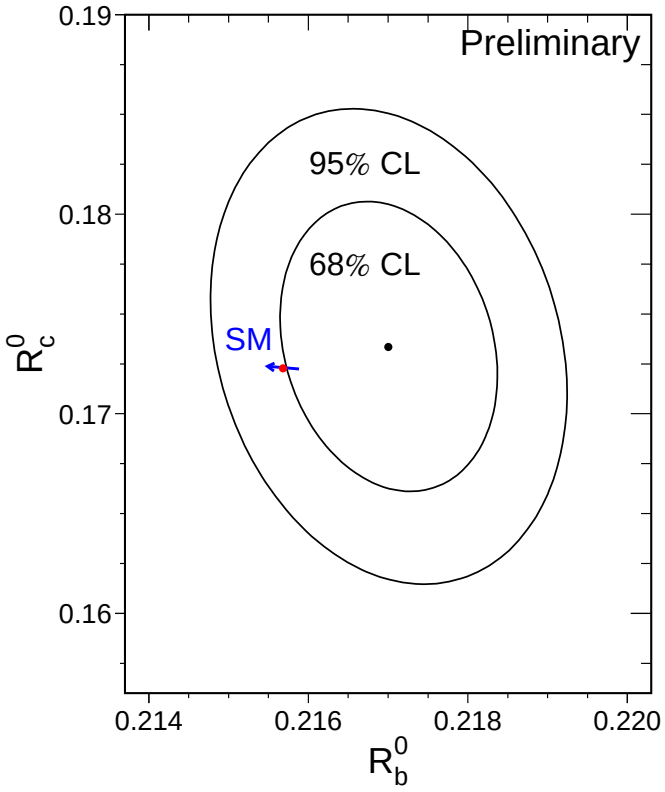


Fig. 4. Contours in the $R_{\rm b}^0 - R_{\rm c}^0$ plane derived from the LEP and SLD heavy flavor results. The arrow indicates the Standard Model expectation for $m_{\rm t} = 175 \pm 5.5$ GeV.

## 2.4 Asymmetries and the Effective Mixing Angle

The measurement of asymmetries, $A_{\rm FB}$ for leptons and $\mathcal{A}_{\rm e}$, $\mathcal{A}_\tau$ from $\tau$ polarization, can be interpreted in terms of the effective mixing angle $\sin^2\theta_{\rm eff}^{\rm lept}$ [Eq. (9)]. The $A_{\rm FB}$ for b and c quarks, as well as inclusive hadrons, can be used under an assumption that the hadronic coupling $\mathcal{A}_{\rm q}$ can be well determined from the Standard Model. The partial widths also have sensitivity through $g_{V{\rm f}}^2$ but the $\mathcal{A}_{\rm f}$'s are related more directly.

A summary of LEP and SLD[7] measurements (many of them preliminary) on $\sin^2\theta_{\rm eff}^{\rm lept}$ is shown in Fig. 5. The most precise measurements are from $A_{\rm FB}^{0,{\rm b}}$, and from $A_{\rm LR}$ by SLD, and agreement between these parameters is not very great. This would be an issue to be followed in the future, in particular after further improvement of $A_{\rm LR}$ from SLD and finalization of the LEP $A_{\rm FB}^{0,\ell}$.

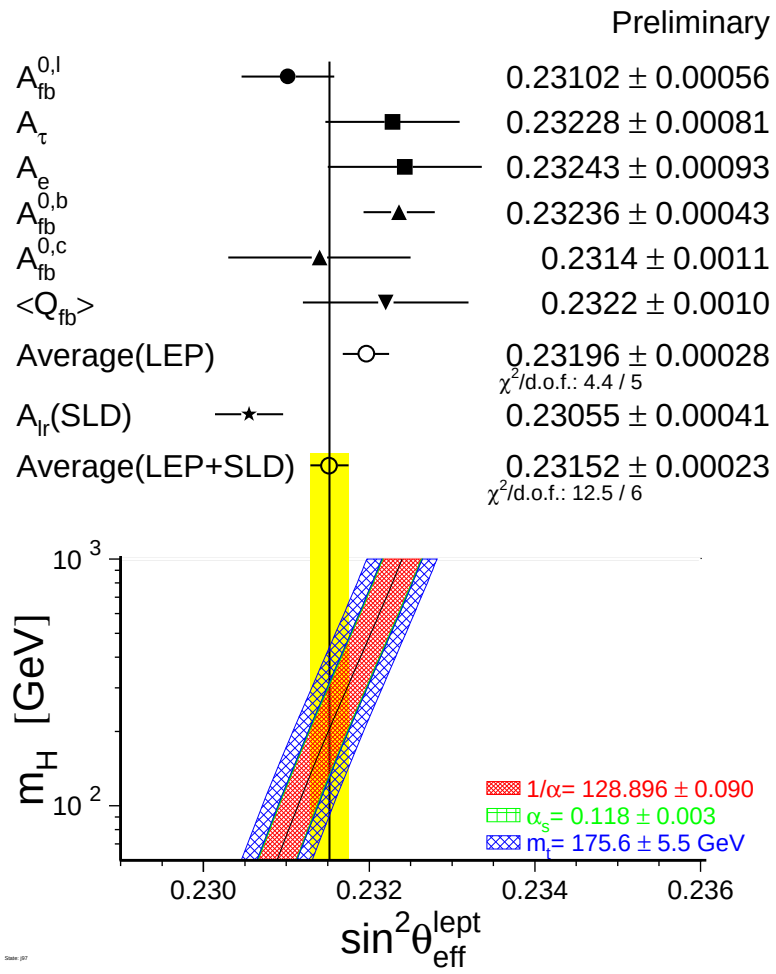


Fig. 5. A summary of $\sin^2\theta_{\rm eff}^{\rm lept}$ from several different asymmetry measurements, compared to the Standard Model expectation as a function of $m_{\rm H}$.

# 3 Fermion Pair Production Above $Z^0$

Fermion pair production in $e^+e^-$ collisions is one of the basic processes of the Standard Model, and deviations from the expected value could be an indication of new physics. At LEP, data were collected at 130–140 GeV (1995), 161 GeV and 171 GeV (1996), and 182 GeV (1997). These energies are well above the $Z^0$ resonance. A feature at these energies is a tendency of radiative return to the $Z^0$ by emitting one or more high-energy photons, reducing the effective center-of-mass energy, $\sqrt{s'}$, of the subsequent $e^+e^-$ collision to a region of the $Z^0$ resonance. Separation can be made between such radiative events and nonradiative events (for which

$\sqrt{s'} \approx \sqrt{s}$) using kinematic information about the final state particles to estimate $s'$ and selecting events above a certain $s'$ (chosen typically at $\sqrt{s'/s} = 0.8$–$0.9$, depending on the collaboration). Figure 6 shows an example of a reconstructed $\sqrt{s'}$ distribution for hadronic events. There are two clear peaks at $\sqrt{s'} = m_{\mathrm{Z}}$ due to the radiative return and the full energy nonradiative events at $\sqrt{s'} \approx \sqrt{s}$, and there is also a nonnegligible fraction of events in between the two peaks and below $m_{\mathrm{Z}}$.

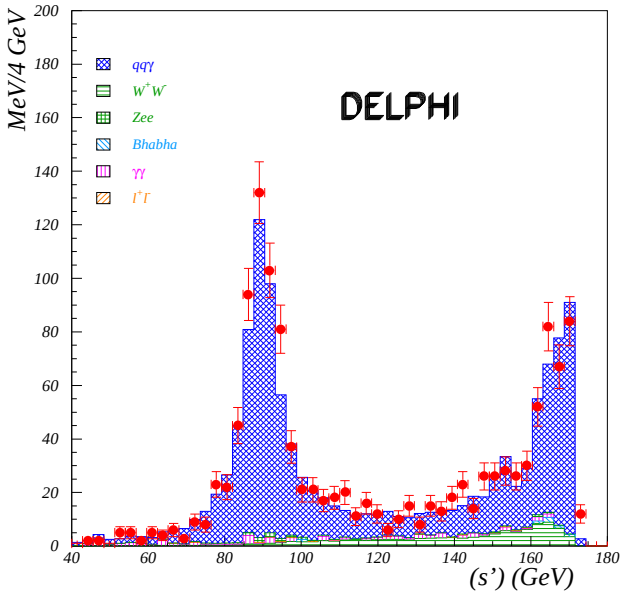


Fig. 6. Distribution of reconstructed effective center-of-mass energy $s'$ for the hadronic events.

There is some ambiguity in the definition of $s'$. The concept of "effective center-of-mass energy after the initial state radiation" is not strict because of the interference between initial and final state photon radiation. In the analysis of OPAL,[8] a prescription was developed to correct the measurement (both total cross section and angular distribution) so that the results can be compared to the theoretical prediction with the initial-final interference switched off. The size of such a correction is small for the inclusive events, but is 1–2% for the nonradiative events.

Cross sections for hadronic and lepton pair final states are shown in Fig. 7, and the leptonic forward-backward charge asymmetry in Fig. 8 for the nonradia-

tive events and the inclusive sample, and are compared to the expectations of the Standard Model. All these measurements are in good agreement with the Standard Model expectation. Cross sections for flavor-tagged quark pair production have also been made.[8,9]

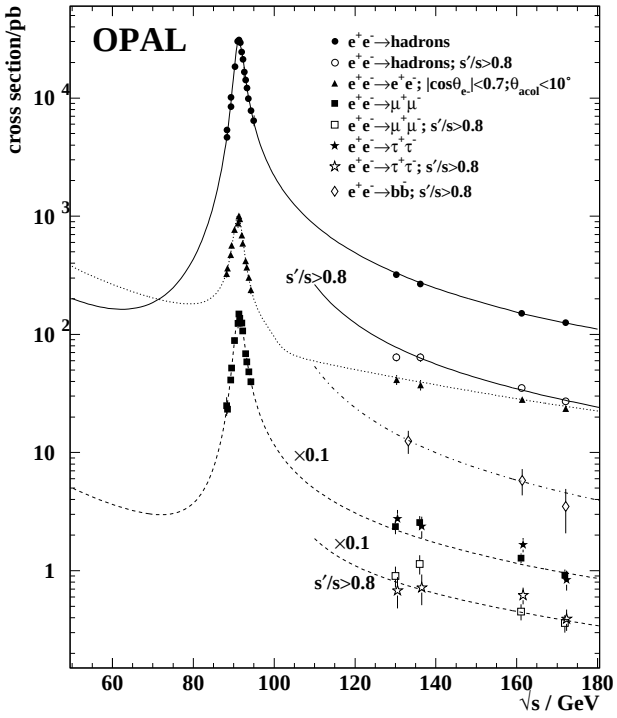


Fig. 7. Measured cross sections for hadronic and leptonic events at LEP-2 energies, for nonradiative and inclusive events.

In the lineshape fits at the $Z^0$ energies, the hadronic $\gamma-Z$ interference is constrained to the Standard Model value. The contribution of $\gamma-Z$ interference to the hadronic cross section is small, and given the parameters of the $Z^0$ it is not excessively model-dependent to use the Standard Model for calculating this effect. Another problem is that the quark couplings to $Z^0$ are not individually determined for each quark flavor from the data. The S-matrix approach[10] is one of the ways to treat the $Z^0$ resonance in a less model-dependent manner. The parameter $j^{\rm tot}_{\rm had}$ determines the overall size of the $\gamma-Z$ interference contribution to the hadronic total cross section. A lineshape fit using this parameterization yields a large uncertainty on the mass of $Z^0$, due to a strong anticorrelation (–75%) between $m_Z$ and $j^{\rm tot}_{\rm had}$. This arises from the energy dependence of the interference term, which

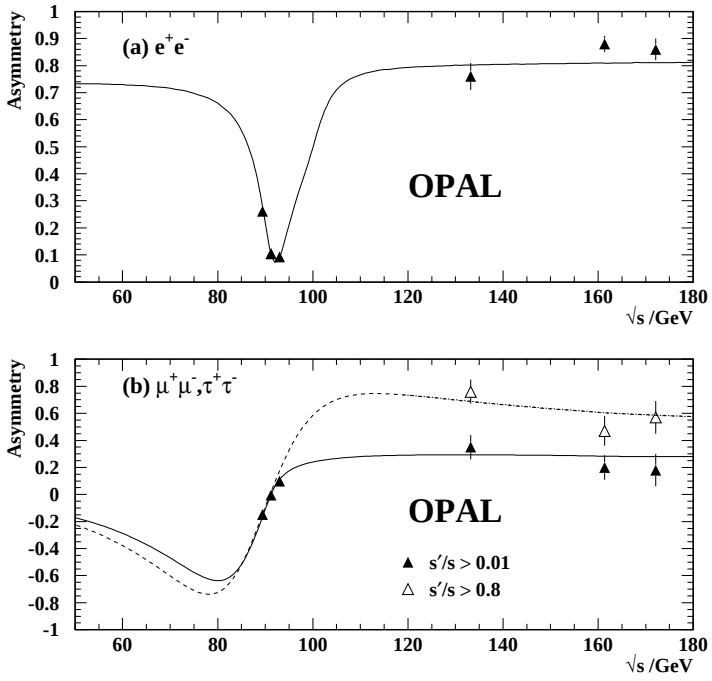


Fig. 8. Measured forward-backward asymmetries of lepton pairs at LEP-2 energies, for nonradiative events (open triangles) and inclusive events (solid triangles) for (a) $e^+e^-$ and (b) $\mu^+\mu^-$, $\tau^+\tau^-$.

changes sign below and above the $Z^0$ resonance. The measurements of nonradiative events at LEP-2, where $\sqrt{s'}$ is well apart from the $Z^0$ resonance, can be used to constrain the interference term. Results of S-matrix fits from the four LEP collaborations using the cross sections and lepton asymmetries at the $Z^0$ energies and LEP-2 energies (130–140, 161, and 172 GeV) are combined[6] and result in $j^{\rm tot}_{\rm had} = 0.14 \pm 0.14$. Hadronic cross sections well below the $Z^0$ peak are also useful to constrain $j^{\rm tot}_{\rm had}$. A measurement at $\sqrt{s} = 55.77$ GeV by the TOPAZ Collaboration[11] at TRISTAN is combined with the LEP results to yield $j^{\rm tot}_{\rm had} = 0.14 \pm 0.12$ (LEP-1 + LEP-2 + TOPAZ), which is consistent with the Standard Model value of $j^{\rm tot}_{\rm had} = 0.22$.

The cross sections and lepton asymmetries for nonradiative events can be used to measure the value of the electromagnetic coupling constant at high energies. The $\alpha_{\rm em}$ determined from fits to the measurements at different center-of-mass energies is shown in Fig. 9 as a function of the energy scale.[8,12] The data are

consistent with the running of $\alpha_{\rm em}$. The LEP-2 data provide the measurements at highest energies. At the highest energy $1/\alpha_{\rm em}(172\ {\rm GeV}) = 127^{+4.0}_{-3.6}$.

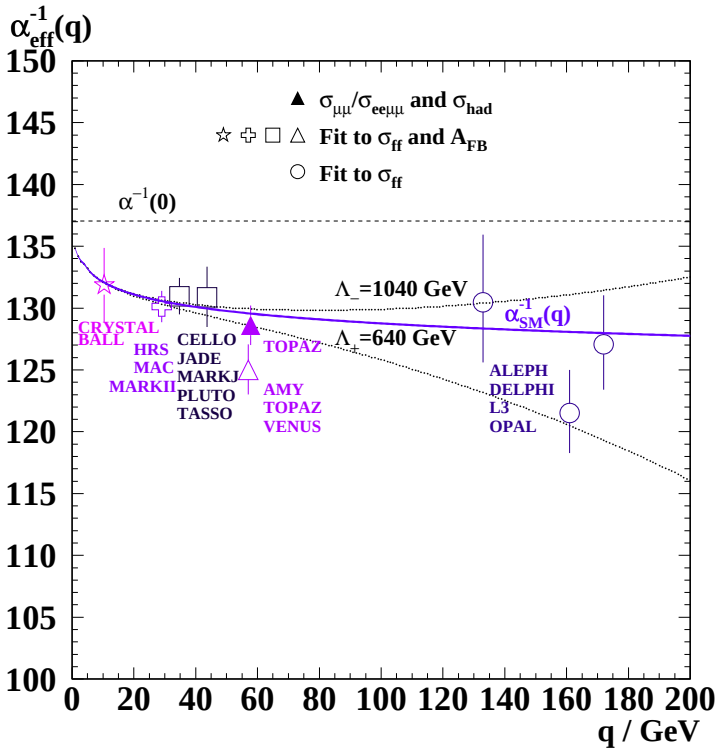


Fig. 9. Electromagnetic coupling constant determined from the cross section and lepton asymmetry as a function of energy. The solid curve indicates the Standard Model calculation.

The high-energy data have been used to search for possible indications of new physics. Searches for Z′, leptoquarks, squarks, and sneutrinos in R-parity breaking SUSY models are performed and limits on the parameters obtained.[8,13,14]

A most general framework for searching for new physics at large-energy scales is the four-fermion contact interaction. Sensitivity to such contact interactions increases as the center-of-mass energy. The LEP collaborations have performed analyses using the LEP-2 fermion pair results and have obtained limits on the energy scale $\Lambda$ in the range of 2–10 TeV, depending on the contact interaction models considered.[8,14]

# 4 The W Bosons

Production of W pairs is a totally new feature at LEP-2. The study of W pair production provides information on two important issues of the Standard Model: determination of the mass of the W boson, and the structure of the triple gauge boson couplings.

In the Standard Model, given a set of experimentally measured parameters, $\alpha$, $G_\mu$, and $m_{\rm Z}$, all other electroweak observables are calculated (or constrained). The mass of the W boson is related to these parameters by the relation

$$G_\mu \;=\; \frac{\alpha\pi}{\sqrt{2}m_{\rm W}^2(1-m_{\rm W}^2/m_{\rm Z}^2)}\cdot\frac{1}{1-\Delta r(m_{\rm t},m_{\rm H},...)}. \qquad (25)$$

The $\Delta r$ represents the radiative correction to the tree-level relation, and depends, in particular, on $m_{\rm t}$ and $m_{\rm H}$. Under the Standard Model constraints, the mass of the W boson has been indirectly determined from global fits to the lower energy measurements, in particular, the precision results from LEP and SLD, to a precision of $\pm 40$ MeV. These constraints become useful with a precise determination of $m_{\rm W}$ to test the Standard Model, and eventually provide information on the yet unknown parameter $m_{\rm H}$.

The W boson pair is produced in $\rm e^+e^-$ collisions either via the $t$-channel $\nu_{\rm e}$ exchange, or $s$-channel $\rm Z^0/\gamma$ exchange, as shown in Fig. 10. The latter diagram involves triple gauge boson couplings (TGC). The TGC in the Standard Model have a specific structure. Any deviation from this causes, in general, a bad high-energy behavior of the cross section, violating unitarity. Observation of such an anomalous coupling would be a signature of new physics beyond the Standard Model.

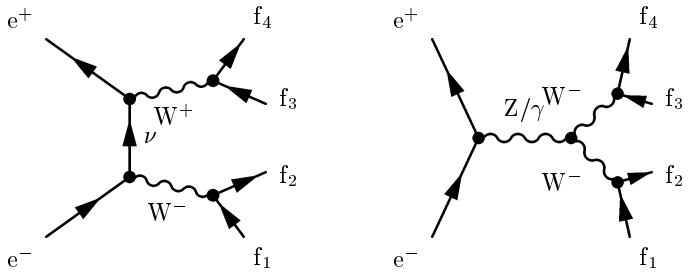


Fig. 10. Feynman diagrams for a four-fermion final state via W pair production.

At LEP-2, both of these issues are addressed. Before the start of LEP-2, $m_{\rm W}$ had been directly measured only at the $\rm p\overline{p}$ colliders.[15] At LEP-2, $m_{\rm W}$ is measured using different techniques in the different environment of the $\rm e^+e^-$ collisions. The cross-section and angular distributions of pair-produced W bosons and their decay products are measured to test the triple gauge couplings. In addition, given the clean sample of W bosons, a study can be made of the basic properties of the W boson ($\Gamma_{\rm W}$, decay branching ratios, ...), as well as the QCD-related studies in the circumstance of four-quark final states, which involves new subjects like color reconnection.

## 4.1 W Pair Events in $\rm e^+e^-$ Collisions

The double-resonant W pair diagram is a major contribution to the four-fermion final states in $\rm e^+e^-$ collisions at the LEP-2 energy. The concept of "W pair production" is not unambiguous. There are other diagrams which produce the same four-fermion final state and they interfere with the W pair diagrams (referred to as the CC03 diagram).[16] However, in the kinematical region where the four fermions look like they are coming from a W pair (i.e., the invariant masses of the two fermion pairs are close to $m_{\rm W}$), the contribution of background diagrams and effect of interference are generally rather small. This allows interpretation of W pair production in terms of the CC03 diagrams.

A W boson decays either hadronically ($\rm q\overline{q}$) or leptonically ($\ell\nu_\ell$). Pair production of $\rm W^\pm$ leads to three classes of final states: (1) hadronic ($\rm q\overline{q}q\overline{q}$), (2) semileptonic ($\rm q\overline{q}\ell\nu$), and (3) leptonic ($\ell\nu\ell\nu$) modes. W pair events are selected according to the characteristics of these three topologies.

1. The hadronic mode composes about 45% of W pair events. These events are characterized by four hadronic jets with no missing energy/momentum. The main background is from the $\gamma/\rm Z^0 \to q\overline{q}$ events, faking four-jet topology due to gluon radiation. For an efficient rejection of background, while keeping the efficiency for W pair events high, analyses are based on the use of likelihood-of-the-event properties or an artificial neural network. Typical event selection efficiency for the 172 GeV sample is about 80% with signal purity of 80%.
2. About 44% of the W pair events are in the semileptonic mode. The $\rm q\overline{q}e\nu$ and $\rm q\overline{q}\mu\nu$ final states are characterized by a two well-separated hadronic jets and a high-momentum lepton. These are associated with a large missing

momentum due to the unobserved neutrino. In the case of the $q\bar{q}\tau\nu$ channel, the $\tau$ is identified as a low multiplicity jet typically consisting of one or three tracks. The missing momentum is less well-defined due to the additional neutrinos from $\tau$ decay. Typical event selection efficiency for $e\nu$ and $\mu\nu$ channels is around 90% and the signal purity over 90%. Performance for the $\tau\nu$ channel is somewhat lower.

3. The remaining 11% of W pair events is purely leptonic. The leptonic decay event consists of two acoplanar, high-momentum leptons with significant missing momentum.

The overall efficiency for the W pair event selection is at the level of 80%. Each LEP collaboration has collected roughly 30 WW candidates at $\sqrt{s}$ = 161 GeV, and 110 at $\sqrt{s}$ = 172 GeV. The integrated luminosity is roughly 10 $pb^{-1}$ per experiment for each of the energy points.

## 4.2 WW Cross Section and Branching Ratios

From the selected number of W pair candidates, the cross section for W pair production is measured at 161 GeV (Refs. 17–20), and 172 GeV (Refs. 21–24).

The LEP averaged W pair cross-section is:[6]

| $\sqrt{s}$ (GeV) | $\sigma_{WW}$ (pb) |
|---|---|
| 161.3 | 3.69 ± 0.45 |
| 172.1 | 12.0 ± 0.7 |

Here, the measurements have been corrected to correspond to the CC03 diagram. In calculating the total cross section, the branching ratio to each of the W decay channels is fixed at the Standard Model value. Figure 11 shows the measured LEP average WW cross section as a function of center-of-mass energy, and compared to the Standard Model expectation, calculated using the GENTLE program. Also shown are the expectations in two extreme cases of anomalous W pair production mechanisms. These are clearly incompatible with the experimental result.

The W decay branching ratios are obtained by fitting the expected number of events for each of the final state modes using a parameterization as a function of decay branching ratios. The LEP average values[6] from the data sets of 161 GeV and 172 GeV are summarized in the table below:

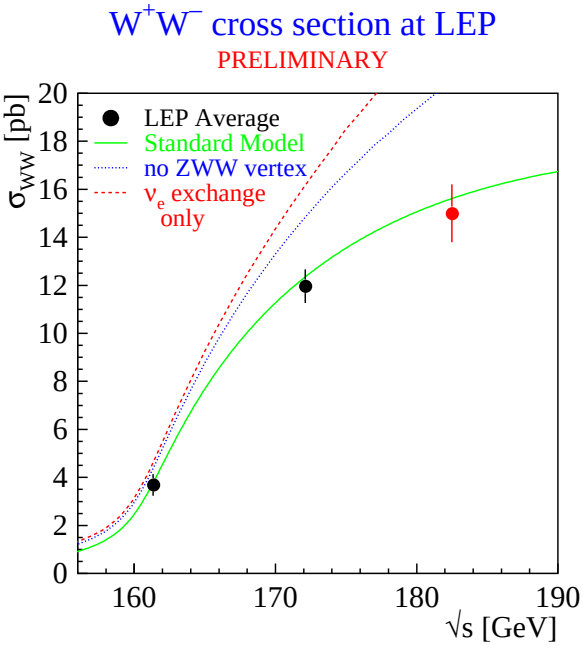


Fig. 11. The cross section for W pair production as a function of center-of-mass energy. The data points are the LEP average. The preliminary result, based on a part of the 183 GeV data, is also shown. Also shown are the Standard Model prediction, and the cases when the ZWW coupling does not exist, or when only $t$-channel $\nu$ exchange exists.

| Decay channel | Branching ratio (%) |
|---|---|
| W$\to$ e$\nu$ | 10.8 $\pm$ 1.3 |
| W$\to \mu\nu$ | 9.2 $\pm$ 1.1 |
| W$\to \tau\nu$ | 12.7 $\pm$ 1.7 |
| W$\to$ q$\overline{\text{q}}$ | 67.2 $\pm$ 1.7 |

The branching ratios for the three lepton species are consistent with each other. The hadronic branching ratio has been determined assuming lepton universality.

From the hadronic decay branching ratio, one can infer the Cabibbo-Kobayashi-Maskawa (CKM) matrix element $V_{cs}$, which is the least well-determined from the earlier measurements. The CKM matrix elements $V_{ij}$ are related to the hadronic branching ratio by

$$\frac{B(\mathrm{W} \to \mathrm{q\overline{q}})}{1 - B(\mathrm{W} \to \mathrm{q\overline{q}})} = (1 + \frac{\alpha_s}{\pi}) \sum_{i=\mathrm{u,c}, j=\mathrm{d,s,b}} |V_{i,j}|^2. \qquad (26)$$

Using the known values[25] of $|V_{ud}|^2 + |V_{us}|^2 + |V_{ub}|^2 + |V_{cd}|^2 + |V_{cb}|^2 = 1.05 \pm 0.01$, one obtains $|V_{cs}| = 0.96 \pm 0.08$. This does not require unitarity of the CKM matrix and can be compared to the existing value from D meson decay of $|V_{cs}|^2 = 1.01 \pm 0.18$.

In addition to this indirect determination, attempts are made for direct measurements of $|V_{cs}|$ using quark flavor tagging in the hadronic W pair events to determine the fraction $R_{\rm cs}$ of the W$\to$ cs decay relative to W$\to$ hadrons, thus extracting $|V_{cs}|$. Results from such LEP measurements are summarized below.[26]

| | $R_{\rm cs}$ | $\lvert V_{cs}\rvert$ |
|---|---|---|
| ALEPH | $0.57 \pm 0.18 \pm 0.04$ | $1.13 \pm 0.43 \pm 0.03$ |
| DELPHI | $0.42 \pm 0.13 \pm 0.06$ | $0.87 \pm 0.24 \pm 0.11$ |

## 4.3 Anomalous Triple Gauge Boson Couplings (TGC)

Pair production of W bosons in $e^+e^-$ collisions involves diagrams of $s$-channel $\gamma$ and $Z^0$ exchange. Observation of W pair production at LEP-2 allows direct tests of the triple gauge boson couplings WW$\gamma$ and WWZ. The most general Lorenz invariant effective Lagrangian which describes the triple gauge boson interaction involves 14 independent parameters:[27] seven for the WW$\gamma$ vertex and seven for the WWZ. It is not practical to experimentally determine all of these 14 parameters. Assuming electromagnetic gauge invariance, C, P, and CP conservation (as in the Standard Model), the number of free parameters is reduced to five. A commonly used set is $(g_1^Z, \kappa_Z, \kappa_\gamma, \lambda_Z, \lambda_\gamma)$. In the Standard Model, the value of these parameters is fixed to $g_1^Z = \kappa_Z = \kappa_\gamma = 1$ and $\lambda_Z = \lambda_\gamma = 0$. Anomalous WW$\gamma$ couplings have been studied at $p\overline{p}$ colliders using the W$\gamma$ final state, and the results are presented in terms of these parameters. Different sets of parameters have also been proposed,[16] motivated by SU(2)×U(1) gauge invariance and constraints already imposed by the precision measurements at $Z^0$. A commonly used set of such parameters is

$$\alpha_{W\phi} = \Delta g_1^Z \cos^2\theta_{\rm W}, \tag{27}$$

$$\alpha_W = \lambda_\gamma, \tag{28}$$

$$\alpha_{B\phi} = \Delta\kappa_\gamma - \Delta g_1^Z \cos^2\theta_{\rm W}, \tag{29}$$

with constraints that $\Delta\kappa_Z = -\Delta\kappa_\gamma \tan^2\theta_{\rm W}$ and $\lambda_Z = \lambda_\gamma$. Here, the parameter with $\Delta$ denotes the deviation of the respective quantity from its Standard Model

value, and $\theta_W$ is the weak mixing angle. All of the $\alpha$ parameters are zero in the Standard Model. These parameters are not well-constrained by the lower energy measurements, and hence are worthwhile to study using W pair production at LEP-2.

Anomalous TGC may affect the total cross section for W pair production as well as the angular distribution of produced W. The relative contributions of each helicity state of the W bosons are also changed, which then affects the distribution of their decay products. Different methods of analyzing the TGC parameter have been developed. One of these is based on the differential distribution of W production on the five angles, production angle of $W^-$, and $W^\pm$ decay angles in the W rest frame. The $q\overline{q}\ell\nu$ mode is most sensitive, since the direction of $W^-$ can be identified using the charge of the lepton. The observed differential distributions are fitted using samples of Monte Carlo simulated events generated with different values of the $\alpha$ parameters in order to determine the best fitted value and its error for each $\alpha$ parameter. The total production cross section is also used to constrain the anomalous coupling. Another method uses a fewer number of optimal observables $\mathcal{O}$, which are constructed from the observed kinematic variables in such a way that $\mathcal{O}_i$ is most sensitive to the deviation of the parameter $\alpha_i$ from its Standard Model value.

A summary of combined[6] LEP measurements of the three $\alpha$ parameters is tabulated in Table 5. In the analysis of each $\alpha_i$, the value of the other parameters is set to the Standard Model value of zero. The combined LEP results were obtained by adding the log-likelihood curves from the four collaborations. Figure 12 shows the log-likelihood curves for the $\alpha_{W\phi}$ fit.

Table 5. The measured values and one-standard deviation errors obtained by the four LEP experiments for the anomalous TGC parameters.

| | $\alpha_{W\phi}$ | $\alpha_W$ | $\alpha_{B\phi}$ |
|---|---|---|---|
| LEP 1-$\sigma$ | $0.02^{+0.16}_{-0.15}$ | $0.15^{+0.27}_{-0.27}$ | $0.45^{+0.56}_{-0.67}$ |
| LEP 95% C.L. | $[-0.28,\ 0.33]$ | $[-0.37,\ 0.68]$ | $[-0.81,\ 1.50]$ |

Constraints on the anomalous TGC can also be obtained at LEP-2 from the study of single W production.[28] One of the diagrams for the We$\nu$ event shown

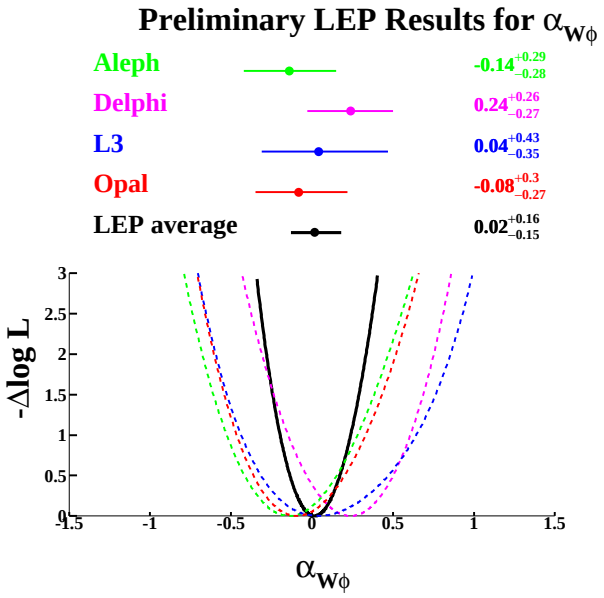


Fig. 12. Log-likelihood curves from $\alpha_{W\phi}$ fits.

in Fig. 13 involves the WW$\gamma$ coupling. Due to the $t$-channel photon exchange, the electron is produced in a small angle, in most cases in the beam pipe, and is therefore invisible. The signature of such single W events is either an acoplanar two jets in case of hadronic decay of the W, or a single high-momentum lepton in the detector in case of leptonic W decay. In both cases, a large missing energy and missing transverse momentum are associated. The cross section for this process is rather small, but the sensitivity of the cross section on the anomalous coupling is large. Another advantage is that this process involves only the WW$\gamma$ coupling, which is complementary to the analysis of W pair events, where both WW$\gamma$ and WWZ couplings are involved. Limits obtained from the single W analyses[29] are tabulated in Table 6.

Table 6. The 95% C.L. limits on the TGC parameters from the analyses of single W events at $\sqrt{s} = 161$ and 172 GeV.

| | | |
|---|---|---|
| L3 | $-3.6 < \Delta\kappa_\gamma < 1.5$ | $-3.6 < \lambda_\gamma < 3.6$ |
| OPAL (preliminary) | $-3.6 < \Delta\kappa_\gamma < 1.6$ | $-3.1 < \lambda_\gamma < 3.1$ |

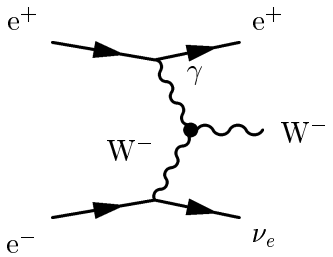


Fig. 13. A Feynman diagram for single W production which involves WW$\gamma$ coupling.

## 4.4 W Mass

The mass of the W has been measured at LEP-2 using two largely different methods. One uses the center-of-mass energy dependence of the W pair cross section near the threshold. The other method, used at higher energy, is based on direct reconstruction of the invariant mass of the W decay products.

### 4.4.1 Threshold Measurement at 161 GeV

Near the production threshold, the cross section for W pair production rises rapidly as the center-of-mass energy rises. Given the Standard Model prediction of the cross section as a function of center-of-mass energy, this allows us to determine the mass of W from the measurement of the cross section. The sensitivity of such a $m_{\rm W}$ measurement is highest at a value of $\sqrt{s}$ roughly 1 GeV above the nominal production threshold. The center-of-mass energy of 161 GeV was chosen for this reason.

Figure 14 shows the $m_{\rm W}$ dependence of the W pair cross section (CC03) at $\sqrt{s} = 161.33$ GeV, calculated using the GENTLE program.[30] The LEP average cross section is indicated by a horizontal band. From this comparison, $m_{\rm W}$ is determined to be

$$m_{\rm W} \;=\; 80.40^{+0.22}_{-0.21} \pm 0.03 \text{ GeV}. \tag{30}$$

The first error is experimental, and the second error is due to uncertainty on the LEP beam energy.

As mentioned before, in a precise sense, the W pair production is a part, though a major part, of general four-fermion production which involves a large

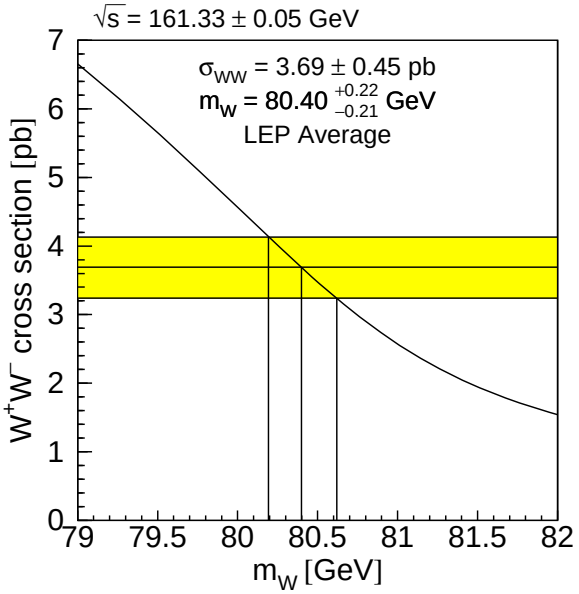


Fig. 14. The CC03 cross section for W pair production as a function of $m_{\mathrm{W}}$ at $\sqrt{s} = 161$ GeV. The horizontal band shows the LEP average cross section. The curve is the Standard Model prediction.

number of interfering diagrams. In the analyses presented above, the effect of interference has been evaluated (these are small) and in some cases corrected. The OPAL Collaboration presented a full four-fermion approach[20] of the threshold measurement of $m_{\mathrm{W}}$. The expected number of selected events are calculated as a function of $m_{\mathrm{W}}$ using a Monte Carlo sample generated by the grc4f program,[31] as shown in Fig. 15. This is an event generator which takes into account all relevant diagrams and interference between them for the four-fermion final state. In this way, any $m_{\mathrm{W}}$ dependence of interference effects and background four-fermion contributions are automatically accounted for. Possible dependence of the event selection efficiency on $m_{\mathrm{W}}$ is also taken into account. The $m_{\mathrm{W}}$ result from the full four-fermion approach is

$$m_{\mathrm{W}} \;=\; 80.40 \pm 0.47 \quad \mathrm{OPAL}\;\; 4-\mathrm{f}, \tag{31}$$

which is in good agreement with the result from the CC03 analysis

$$m_{\mathrm{W}} \;=\; 80.40 \pm 0.47 \quad \mathrm{OPAL}\;\; \mathrm{CC03}. \tag{32}$$

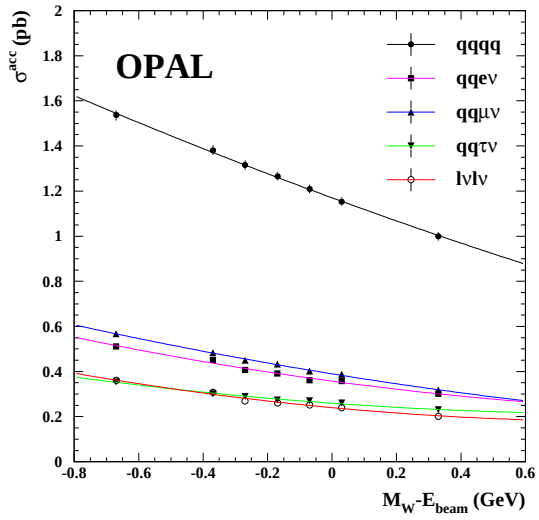


Fig. 15. The OPAL accepted cross section for four-fermion events at 161 GeV, as a function of $m_{\mathrm{W}}$. The points are calculated using the grc4f generator at seven different values of $m_{\mathrm{W}}$. The parameterization indicated by the curves is used to fit $m_{\mathrm{W}}$.

### 4.4.2 Direct Reconstruction Above Threshold

At higher energies, $m_{\mathrm{W}}$ is determined based on an event-by-event estimator of the W boson mass, evaluated from the invariant masses of W decay products. Events in the hadronic mode and semileptonic mode are used. The analysis goes in general in the following way.

For the $\mathrm{q\overline{q}q\overline{q}}$ events, particles are combined into four jets. The energy and momentum of each jet are evaluated. In the case of $\mathrm{q\overline{q}}\ell\nu$ events, the momentum of the identified charged lepton and the energy and momentum of the two hadronic jets are measured.

The resolution of these measurements, in particular the jet energy, is improved by kinematic fits requiring four-momentum conservation. The total energy is constrained by the LEP beam energy. The kinematic fit also helps to reduce sensitivity of the measured invariant mass to the error on the absolute scale of measured jet/lepton energies. For the $\mathrm{q\overline{q}q\overline{q}}$ mode, four-momentum conservation leads to a fit with four-constraints (4C-fit), while the $\mathrm{q\overline{q}}\ell\nu$ mode yields a 1C-fit due to three unknown quantities of the neutrino. An additional constraint can

be imposed requiring equality of two invariant masses, leading to a 5C-fit for the $q\bar{q}q\bar{q}$ mode and a 2C-fit for the $q\bar{q}\ell\nu$ mode, and a single mass-estimator is used for the analysis. In the case of the $q\bar{q}\tau\nu$ mode, the momentum of the $\tau$ cannot be measured; only the approximate $\tau$ direction can be determined. Instead of a kinematic fit, a simple jet energy rescaling to the beam energy is often used for the $q\bar{q}\tau\nu$ mode.

A complexity in the $q\bar{q}q\bar{q}$ mode is the ambiguity of jet pairing. There are three possible combinations in choosing two pairs of jets out of the four jets. The closeness of the two invariant masses, or, in a 5C-fit, the $\chi^2$ probability with an equal mass constraint is used to choose the most likely jet pairs. The second most probable candidate is also used for the analyses in certain conditions. In general, incorrect pairing tends to lead to a rather uniform distribution of the reconstructed invariant mass.

Another problem in the $q\bar{q}q\bar{q}$ mode arises from the final state hadronic interaction. Since the time scale of hadronization is longer than the lifetime of the W boson, hadronization of quarks from different W bosons may not be independent. This is referred to as the "color reconnection" problem. The effect of the Bose-Einstein correlation between identical bosons from different W boson decays is another possible source of bias in the reconstructed W mass. According to earlier studies of such effects,[16] a bias on the W mass measurement using the $q\bar{q}q\bar{q}$ channel may be as large as 100 MeV. There is as of yet no definite theoretical prediction of such effects available. This size of uncertainty on $m_{\mathrm{W}}$ is associated with the measurement using the hadronic mode. There have been a number of attempts to assess such effects experimentally. At this stage, the available LEP-2 W pair sample is rather small. As the data increases in the future, the significance of such studies will also increase.

In order to determine $m_{\mathrm{W}}$ from the observed invariant mass distribution, a number of different techniques have been developed by the four LEP collaborations.[21–24]

- The observed invariant mass distribution is fitted using a simple analytic function. The Breit-Wigner distribution is a natural choice to describe a resonance. Contributions from background processes and from incorrect pairing in the $q\bar{q}q\bar{q}$ mode produces a rather smooth distribution, and can also be parameterized using a simple analytic function. The peak position of the Breit-Wigner signal distribution is used as the estimator of $m_{\mathrm{W}}$. This value is in

general shifted by a few 100 MeV from the true value for a number of reasons: Initial state radiation (ISR), detector resolution, and other effects combined with the constrained kinematic fit result in the reconstructed mass distribution being distorted from the true distribution. Such bias is calibrated using Monte Carlo samples generated with different values of $m_{\mathrm{W}}$. An example of such fits is shown in Fig. 16. This method is used as a cross-check of the result obtained by the main methods described below.

- If the observed mass distribution is fitted using a function which takes into account all of the experimental effects and those of physics origin (like ISR), the $m_{\mathrm{W}}$ so extracted is expected to be unbiased. A method used by ALEPH, L3, and OPAL is based on constructing such an expected distribution as a function of $m_{\mathrm{W}}$ using Monte Carlo samples with full detector simulation. All the experimental procedures—event selection and kinematic fits—are applied to the Monte Carlo sample of signal and background. The obtained Monte Carlo distribution is used to fit the observed data distribution. This method requires a large number of Monte Carlo samples generated with different values of $m_{\mathrm{W}}$. In practice, a Monte Carlo distribution for an arbitrary value of $m_{\mathrm{W}}$ is constructed by weighting each event according to the ratio of cross sections for producing two W bosons of the masses $(m_1, m_2)$ when the W boson mass is $m_{\mathrm{W}}$ and the reference value $m_{\mathrm{W}}^0$, which is used for generating the Monte Carlo sample. Then, a likelihood of observing the data distribution is evaluated as a function of $m_{\mathrm{W}}$, and the best fit value of $m_{\mathrm{W}}$ and its error is extracted. This method can be easily extended to also fit the total width of the W boson, $\Gamma_{\mathrm{W}}$. Such two-dimensional fits yield:[23,24]

$$\Gamma_{\mathrm{W}} = 1.74^{+0.88}_{-0.78} \pm 0.25 \quad \text{(L3)}, \tag{33}$$

$$\Gamma_{\mathrm{W}} = 1.30^{+0.62}_{-0.55} \pm 0.18 \quad \text{(OPAL)}, \tag{34}$$

  where the first error is statistical and the second systematic.

- DELPHI developed a method in which the information on $m_{\mathrm{W}}$ is extracted from the likelihood of observing each individual event. It takes into account the event-by-event invariant mass resolution, an attempt to make optimal use of available experimental information, thus improving the statistical precision of the measurement. This method requires calibration for overall bias on the extracted $m_{\mathrm{W}}$.

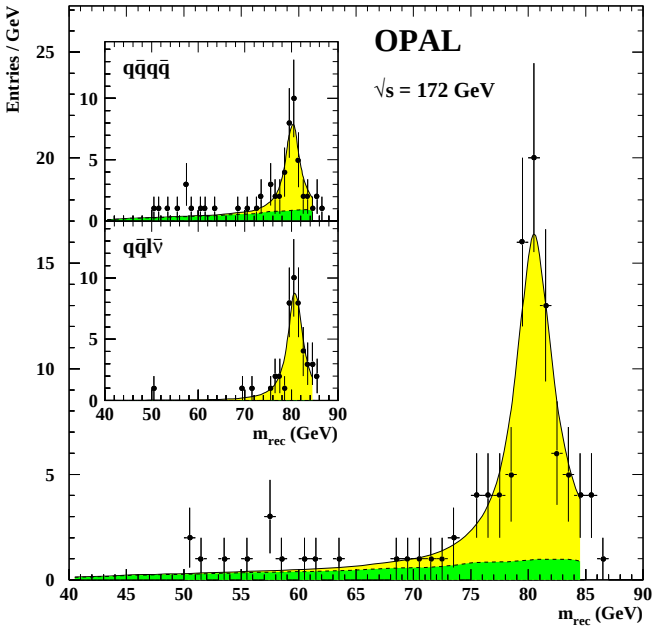


Fig. 16. Reconstructed invariant mass distributions for the $W^+W^-$ candidates. The three plots are for the $q\overline{q}q\overline{q}$ mode, $q\overline{q}\ell\nu$ mode, and combined distribution. The points are data and the curve is the parameterization using Breit-Wigner plus polynomial.

The results of $m_{\rm W}$ measurements at 172 GeV by the four LEP collaborations are summarized in Fig. 17, shown separately for the $q\overline{q}\ell\nu$ mode and the $q\overline{q}q\overline{q}$ mode.[6] The common systematic error contains 30 MeV from the LEP beam energy uncertainty, and for the $q\overline{q}q\overline{q}$ mode, an additional 100 MeV due to uncertainty on the effect of color reconnection and Bose-Einstein correlations (ALEPH uses 60 MeV for the latter uncertainty based on their new evaluation).

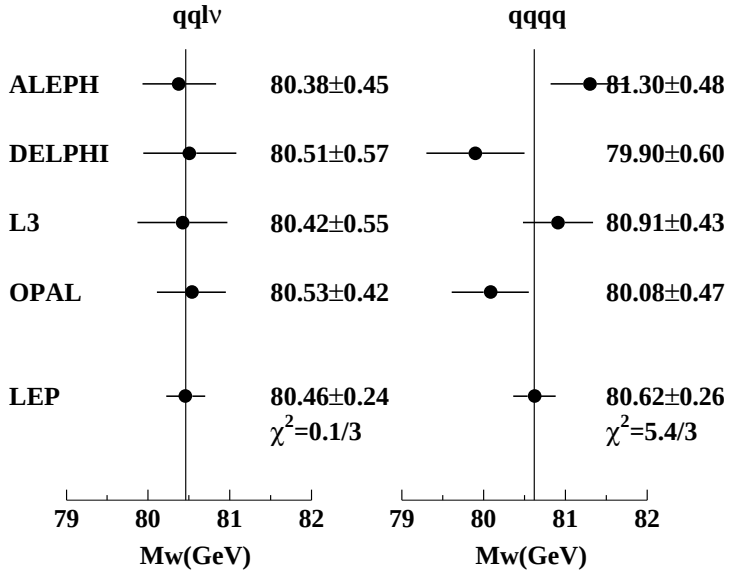


Fig. 17. LEP measurements of $m_{\rm W}$ from the 172 GeV data.

Within the present experimental uncertainty, the $m_{\rm W}$ determined from the $q\overline{q}\ell\nu$ mode and $q\overline{q}q\overline{q}$ mode are consistent with each other, and these are combined to yield the LEP average value from the 172 GeV data of

$$m_{\rm W} \;=\; 80.53 \pm 0.17 \pm 0.05 \quad ({\rm GeV}) \quad (172 \text{ GeV}). \tag{35}$$

Combining this result with that from the 161 GeV data, we obtain the LEP average

$$m_{\rm W} \;=\; 80.48 \pm 0.13 \pm 0.04 \quad ({\rm GeV}) \quad (161 + 172 \text{ GeV}). \tag{36}$$

This result can be compared to the average Tevatron result of $m_{\rm W} = 80.41 \pm 0.09$ GeV (Ref. 32). The precision of the new LEP result is becoming comparable to the Tevatron result, and the two results are consistent with each other.

# 5 The Standard Model

The precision measurements at LEP use a variety of quantities to check the overall consistency of the Standard Model, and within its framework, infer information about its fundamental parameters, in particular the top quark mass $m_{\rm t}$, W mass $m_{\rm W}$, and $\alpha_s(m_{\rm Z}^2)$, for which comparisons are possible with direct measurements, and the unknown mass of the Higgs boson.

This is done by global fits to the LEP precision measurements using the Standard Model.[6] The input data are summarized in Table 7. Also included are results from the SLD Collaboration; $m_{\rm W}$ from the UA2, CDF, and DØ Collaborations; $1-(m_{\rm W}/m_{\rm Z})^2$ from $\nu$N scattering; and the top mass from CDF and DØ. In addition, the electromagnetic coupling constant $\alpha_{\rm em}(m_{\rm Z}^2)$ (Ref. 33) is used in the fit.

A fit using the LEP data only yields the results summarized in column 2 of Table 8. All of the Standard Model parameters, $\alpha_{\rm em}(m_Z^2)$, $m_{\rm t}$, $m_{\rm H}$, and $\alpha_s(m_{\rm Z}^2)$, are allowed to vary. In the fit, $m_{\rm t}$ and $m_{\rm H}$ are correlated, as seen in Fig. 18. One sees that the LEP data prefers lower top quark mass and Higgs mass, though the errors are large. This is mainly due to the still somewhat smaller value of $R_{\rm b}^0$.

The data can be used to determine $m_{\rm t}$ and $m_{\rm W}$ indirectly. Results of such a fit, without using the $m_{\rm t}$ and $m_{\rm W}$ data, are shown in column 3 of Table 8. Figure 19 shows a contour in the $m_{\rm t}-m_{\rm W}$ plane, compared to the direct measurements. Also shown are the Standard Model predictions for the Higgs mass in the range of 60–1000 GeV. The indirect measurements prefer low values of both $m_{\rm t}$ and $m_{\rm H}$.

The third fit uses all data, including $m_{\rm t}$ and $m_{\rm W}$. The overall $\chi^2$/d.o.f is 17/15. The reduced contour in the $m_{\rm t}-m_{\rm H}$ plane is shown in Fig. 18. The dependence of $\chi^2$ as a function of $m_{\rm H}$ is shown in Fig. 19. The width of the band indicates an estimated uncertainty due to the missing higher-order corrections. The one-sided 95% C.L. upper limit on the Higgs mass is 420 GeV. The lower limit of about 77 GeV from the direct searches[34] is also shown (which is not used in the calculation of the upper limit).

The value of $\alpha_s(m_{\rm Z}^2)$ is determined from the fits to be $\alpha_s(m_{\rm Z}^2) = 0.120 \pm 0.003$, which is consistent with the world average[25] of $\alpha_s(m_{\rm Z}^2) = 0.118 \pm 0.003$. The analysis using $R_\ell$ only yields a slightly larger value of $\alpha_s(m_{\rm Z}^2) = 0.124 \pm 0.004 \pm 0.002$, with the second error due to the variation of $m_{\rm H}$ in the range of 60–1000 GeV.

Table 7. Summary of measurements and the Standard Model fit results (column 4). The pulls (difference between measurement and fit in units of the total measurement error) are shown in column 5. In the fit, the Higgs mass is treated as a free parameter. The systematic error on $m_Z$ and $\Gamma_Z$ is due to the LEP energy uncertainty.

| | Measurement with total error | Systematic error | Standard Model | Pull |
|---|---|---|---|---|
| $\alpha(m_Z^2)^{-1}$ | $128.896 \pm 0.090$ | 0.083 | 128.898 | 0.0 |
| <u>LEP</u> | | | | |
| lineshape and $A_{FB}^{\ell}$ | | | | |
| $m_Z$ [GeV] | $91.1867 \pm 0.0020$ | 0.0015 | 91.1866 | 0.0 |
| $\Gamma_Z$ [GeV] | $2.4948 \pm 0.0025$ | 0.0015 | 2.4966 | −0.7 |
| $\sigma_{had}^0$ [nb] | $41.486 \pm 0.053$ | 0.052 | 41.467 | 0.4 |
| $R_\ell$ | $20.775 \pm 0.027$ | 0.024 | 20.756 | 0.7 |
| $A_{FB}^{0,\ell}$ | $0.0171 \pm 0.0010$ | 0.0007 | 0.0162 | 0.9 |
| $\tau$ polarization: | | | | |
| $\mathcal{A}_\tau$ | $0.1411 \pm 0.0064$ | 0.0040 | 0.1470 | −0.9 |
| $\mathcal{A}_e$ | $0.1399 \pm 0.0073$ | 0.0020 | 0.1470 | −1.0 |
| $q\overline{q}$ charge asymmetry: | | | | |
| $\sin^2\theta_{eff}^{lept}$ | $0.2322 \pm 0.0010$ | 0.0008 | 0.23152 | 0.7 |
| $m_W$ [GeV] | $80.48 \pm 0.14$ | 0.05 | 80.375 | 0.8 |
| <u>SLD</u> | | | | |
| $\sin^2\theta_{eff}^{lept}$ $(A_{LR})$ | $0.23055 \pm 0.00041$ | 0.00014 | 0.23152 | −2.4 |
| <u>LEP and SLD H.F.</u> | | | | |
| $R_b^0$ | $0.2170 \pm 0.0009$ | 0.0007 | 0.2158 | 1.3 |
| $R_c^0$ | $0.1734 \pm 0.0048$ | 0.0038 | 0.1723 | 0.2 |
| $A_{FB}^{0,b}$ | $0.0984 \pm 0.0024$ | 0.0010 | 0.1031 | −2.0 |
| $A_{FB}^{0,c}$ | $0.0741 \pm 0.0048$ | 0.0025 | 0.0736 | 0.1 |
| $\mathcal{A}_b$ | $0.900 \pm 0.050$ | 0.031 | 0.935 | −0.7 |
| $\mathcal{A}_c$ | $0.650 \pm 0.058$ | 0.029 | 0.668 | −0.3 |
| <u>$p\overline{p}$ and $\nu N$</u> | | | | |
| $m_W$ [GeV] $(p\overline{p})$ | $80.41 \pm 0.09$ | 0.07 | 80.375 | 0.4 |
| $1-(m_W/m_Z)^2$ $(\nu N)$ | $0.2254 \pm 0.0037$ | 0.0023 | 0.2231 | 0.6 |
| $m_t$ [GeV] $(p\overline{p})$ | $175.6 \pm 5.5$ | 4.2 | 173.1 | 0.4 |

Table 8. Results of the fits to LEP data only, to all data except the direct determinations of $m_{\rm t}$ and $m_{\rm W}$ (Tevatron and LEP-2), and to all data including the top quark mass determination. As the sensitivity to $m_{\rm H}$ is logarithmic, both $m_{\rm H}$ as well as $\log(m_{\rm H}/{\rm GeV})$ are quoted. The bottom part of the table lists derived results for $\sin^2\theta^{\rm lept}_{\rm eff}$, $1-(m_{\rm W}/m_{\rm Z})^2$, and $m_{\rm W}$.

| | LEP including LEP-2 $m_{\rm W}$ | All data except $m_{\rm t}$ and $m_{\rm W}$ | All data |
|---|---|---|---|
| $m_{\rm t}$ (GeV) | $158^{+14}_{-11}$ | $157^{+10}_{-9}$ | $173.1 \pm 5.4$ |
| $m_{\rm H}$ (GeV) | $83^{+168}_{-49}$ | $41^{+64}_{-21}$ | $115^{+116}_{-66}$ |
| $\log(m_{\rm H}/{\rm GeV})$ | $1.92^{+0.48}_{-0.39}$ | $1.62^{+0.41}_{-0.31}$ | $2.06^{+0.30}_{-0.37}$ |
| $\alpha_s(m_{\rm Z}^2)$ | $0.121 \pm 0.003$ | $0.120 \pm 0.003$ | $0.120 \pm 0.003$ |
| $\chi^2$/d.o.f. | 8/9 | 14/12 | 17/15 |
| $\sin^2\theta^{\rm lept}_{\rm eff}$ | $0.23188 \pm 0.00026$ | $0.23153 \pm 0.00023$ | $0.23152 \pm 0.00022$ |
| $1-(m_{\rm W}/m_{\rm Z})^2$ | $0.2246 \pm 0.0008$ | $0.2240 \pm 0.0008$ | $0.2231 \pm 0.0006$ |
| $m_{\rm W}$ (GeV) | $80.298 \pm 0.043$ | $80.329 \pm 0.041$ | $80.375 \pm 0.030$ |

# 6 Summary and Outlook

The LEP-1 program resulted in many important physics results: precise determination of the $\rm Z^0$ parameters, determination of $N_\nu$, and information for valuable tests of the Standard Model. It appears that the data are in excellent agreement with the Standard Model, and with the direct measurements of $m_{\rm t}$ and $m_{\rm W}$. The data collection of $\rm Z^0$ events has finished. There are many results yet to be finalized, which we expect will come soon.

At LEP-2, precise measurements of $m_{\rm W}$ and study of the TGC are making progress, and by the end of the LEP-2 program, the precision of these measurements will reach the expected level. Sensitivity to other processes such as two-fermion and four-fermion production will also increase with the growth of the data sample. For an optimal use of the data, progress is needed on theoretical calculations as well.

Another important issue at LEP-2 is to extend the search of the Higgs boson to around the mass of $\rm Z^0$.

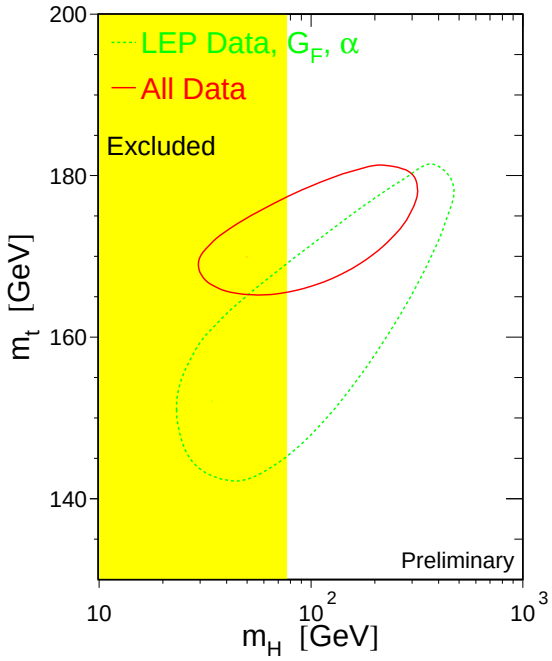


Fig. 18. The 68% probability contours in the $m_{\rm t} - m_{\rm H}$ plane for the fit to the LEP data only (dashed curve) and to all data including CDF/DØ $m_{\rm t}$ measurements (solid curve). The vertical band indicates the range of $m_{\rm H}$ excluded at 95% C.L. by the direct search.

Though it was not discussed in this article, the study of QCD is another major subject at LEP. Based on the large number of high-purity hadronic events from $Z^0$ decay, a variety of QCD tests have been performed, and precision measurements of $\alpha_s$ have been made. LEP-2 provides an extended energy scale, by a factor of two, allowing studies of the energy evolution of $\alpha_s$ and of other hadronic observables.

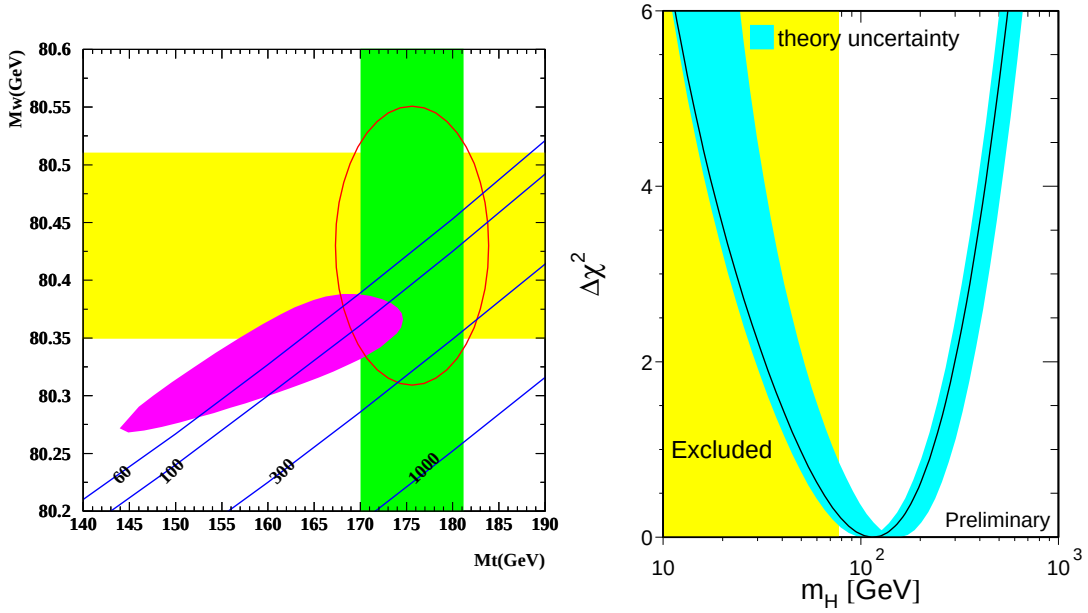


Fig. 19. (a) The 68% probability contour in the $m_{\mathrm{t}} - m_{\mathrm{W}}$ plane for the fit without using $m_{\mathrm{W}}$ and $m_{\mathrm{t}}$ measurements (the filled area). Direct measurements are indicated by the vertical and horizontal bands and also by a 68% C.L. contour. (b) $\Delta\chi^2$ vs $m_{\mathrm{H}}$ for the fit using all the data. The vertical band shows the 95% C.L. exclusion limit from the direct search.

## Acknowledgments

I would like to thank the LEP Collaborations: ALEPH, DELPHI, L3, and OPAL; the LEP/SLD electroweak working groups; the LEP energy working group; and the theory community for the preparation and providing of the physics results presented at the SLAC Summer Institute. I also thank the organizers of the SSI for inviting me to this well-organized and stimulating program.

## References

[1] "Report of the working group on precision calculations for the Z resonance," edited by D. Bardin, W. Hollik, and G. Passarino, CERN Yellow Report 95-03.

[2] The CDF Collaboration, J. Lys, "Top mass measurements at CDF," in *Proceedings of the ICHEP96 Conference* (Warsaw, Poland, 1996), p. 1196;
DØ Collaboration, S. Abachi *et al.*, Phys. Rev. Lett. **79**, 1197 (1997).

[3] The LEP energy working group. Contact person T. Camporesi.

[4] A. Arbuzov *et al.*, Phys. Lett. B **383**, 238 (1996);
S. Jadach *et al.*, Comp. Phys. Comm. **102**, 229 (1997).

[5] D. Bardin *et al.*, Z. Phys. C **44**, 493 (1989); Comp. Phys. Comm. **59**, 303 (1990); Nucl. Phys. B **351**, 1 (1991); Phys. Lett. B **255**, 290 (1991) and CERN-TH 6443/92 (May 1992).

[6] The LEP Collaborations ALEPH, DELPHI, L3, OPAL; the LEP Electroweak Working Group; and the SLD Heavy Flavour Group, "Combination of preliminary electroweak measurements and constraints on the Standard Model," CERN-PPE/97-154. Reference to each of the individual results are given therein.

[7] B. Schumm, these proceedings.

[8] The OPAL Collaboration, K. Ackerstaff *et al.*, CERN-PPE/97-101, accepted by Euro. Phys. Journal.

[9] The DELPHI Collaboration, contributed paper **466** to the EPS-HEP-97, (Jerusalem, Israel).

[10] A. Leike, T. Riemann, and J. Rose, Phys. Lett. B **273**, 513 (1991); T. Riemann, Phys. Lett. B **293**, 451 (1992).

[11] The TOPAZ Collaboration, K. Miyabayashi *et al.*, Phys. Lett. B **347**, 171 (1995).

[12] M. Kobel, FREIBURG-EHEP-97-13, contributed paper to the Lepton-Photon Symposium (Hamburg, Germany, 1997).

[13] The L3 Collaboration, contributed paper **510** to the EPS-HEP-97;
The DELPHI Collaboration, contributed paper **469** to the EPS-HEP-97.

[14] The ALEPH Collaboration, contributed paper **856** to the EPS-HEP-97;
The DELPHI Collaboration, contributed paper **467** to the EPS-HEP-97.

[15] The CDF Collaboration, F. Abe *et al.*, Phys. Rev. Lett. **75**, 11 (1995); The CDF Collaboration, F. Abe *et al.*, Phys. Rev. D **52**, 4784 (1995); The DØ Collaboration, S. Abachi *et al.*, Phys. Rev. Lett. **77**, 3309 (1996); The UA2 Collaboration, J. Alitti *et al.*, Phys. Lett. B **276**, 354 (1992); The UA1 Collaboration, C. Albajar *et al.*, Z. Phys. C **44**, 15 (1989).

[16] *Physics at LEP2*, CERN 96-01, edited by G. Altarelli, T. Sjöstrand, and F. Zwirner.

[17] The ALEPH Collaboration, R. Barate *et al.*, Phys. Lett. B **401**, 347 (1997).

[18] The DELPHI Collaboration, P. Abreu *et al.*, Phys. Lett. B **397**, 158 (1997).

[19] The L3 Collaboration, M. Acciarri *et al.*, Phys. Lett. B **398**, 223 (1997).

[20] The OPAL Collaboration, K. Ackerstaff *et al.*, Phys. Lett. B **389**, 416 (1996).

[21] The ALEPH Collaboration, CERN-PPE/97-102 (submitted to Phys. Lett. B.); The ALEPH Collaboration, contributed paper **600** to EPS-HEP-97 (Jerusalem, Israel).

[22] The DELPHI Collaboration, contributed paper **347** to EPS-HEP-97 (Jerusalem, Israel).

[23] The L3 Collaboration, M. Acciarri *et al.*, Phys. Lett. B **407**, 419 (1997); The L3 Collaboration, M. Acciarri *et al.*, Phys. Lett. B **413**, 176 (1997).

[24] The OPAL Collaboration, K. Ackerstaff *et al.*, Euro. Phys. Journal C **1**, 395 (1998).

[25] The Particle Data Group, R. M. Barnett *et al.*, Phys. Rev. **54**, 1 (1996).

[26] The DELPHI Collaboration, contributed paper **535** to EPS-HEP-97 (Jerusalem, Israel); The ALEPH Collaboration, contributed paper **667** to EPS-HEP-97 (Jerusalem, Israel).

[27] K. Hagiwara *et al.*, Nucl. Phys. **409**, 253 (1987).

[28] T. Tsukamoto and Y. Kurihara, Phys. Lett. B **389**, 162 (1996).

[29] The L3 Collaboration, M. Acciarri *et al.*, Phys. Lett. B **403**, 168 (1997); The OPAL Collaboration, contributed paper to EPS-HEP-97 (Jerusalem, Israel).

[30] D. Bardin *et al.*, Comp. Phys. Comm. **104**, 161 (1997).

[31] J. Fujimoto *et al.*, Comp. Phys. Comm. **100**, 128 (1997).

[32] Y. K. Kim, talk presented at the Lepton-Photon Symposium (Hamburg, Germany, 1997).

[33] S. Eidelmann and F. Jegerlehner, Z. Phys. C **67**, 585 (1995).

[34] P. Janot, talk at EPS-HEP-97 (Jerusalem, Israel, 1997).